CP-2005/02

Effects of Strong-Motion Processing Procedures on Time Histories, Elastic, and Inelastic Spectra

2005

COSMOS
www.strongmotion.org
2443 Fillmore Street #380-6131
San Francisco, CA 94115

Consortium of Organizations for Strong-Motion Observation Systems

C O S M O S

Final Report

Effects of Strong-Motion Processing Procedures on Time Histories, Elastic, and Inelastic Spectra

Sponsors
U.S. Geological Survey
COSMOS

COSMOS
Publication
NO. CP-2005/02

Consortium of Organizations for
Strong-Motion Observation Systems

and

U.S. Geological Survey

Final Report

Effects of Strong-Motion Processing Procedures on Time Histories, Elastic, and Inelastic Spectra

COSMOS Publication
CP-2005/02

Editors

William U. Savage. U. S. Geological Survey

J. Carl Stepp, COSMOS

Claire M. Johnson, COSMOS

Preface

Worldwide, earthquake strong-motion observation networks are being expanded with the continuing addition of strong-motion recording stations. Many thousand strong-motion recordings are now available and the inventory continues to grow. Web-based data dissemination technologies now permit seamless, efficient dissemination of strong-motion data over the Internet by linking multiple independent database providers through a central dissemination hub. The COSMOS Strong-Motion Virtual Data Center (VDC) (http://www.db.cosmos-eq.org) at the University of California, Santa Barbara is leading the development of efficient web-based search and dissemination infrastructure with funding provided by the National Science Foundation, Southern California Earthquake Center, U. S. Geological Survey, California Geological Survey, and COSMOS. Using this infrastructure earthquake professionals can now rapidly obtain strong-motion recordings from participating strong-motion observation networks located anywhere in the world.

To support optimum use of these important advances in strong motion monitoring and data dissemination capabilities by earthquake professionals, standardized formatting and processing of strong-motion recordings is essential. COSMOS has developed a consensus strong motion record formatting standard http://www.cosmos-eq.org/publications , which currently is being implemented by the COSMOS VDC and the California Integrated Seismic Network (CISN), http://www.cisn.org. Additionally, COSMOS has recently completed development of a guideline for strong motion-record processing, http://www.cosmos-eq.org/publications.

The technical information base supporting development of the strong-motion record processing guideline was compiled in a workshop, which reviewed strong-motion record processing experience and current record processing practices of twelve major strong-motion network organizations located in eight nations. To supplement and expand this compilation of record processing practice, COSMOS with funding support provided by the U. S. Geological Survey sponsored the research reported in this publication (*COSMOS Publication No. CP-2005/02*). The research specifically addressed the question: how significant is the variation in the linear and nonlinear response of different structures to the same ground motion records processed with different filtering techniques? An understanding of this question has become of critical importance with the increasing use of nonlinear structural dynamic analysis methods, which allow engineers to now realistically estimate the building response and potential damage resulting from an earthquake recording.

Professor C. Allin Cornell and Dr. David M. Boore provided peer review for this work, reviewing the proposed scope of work, providing feedback and guidance on intermediate results, and providing critical review of the draft final report.

J. Carl Stepp
COSMOS Project Manager

Acknowledgments

The authors are grateful to Professor C. Allin Cornell and Dr. David Boore for their insights and comments that improved the quality of this work, and to Dr. Carl Stepp and Dr. Woody Savage for their support that made this study possible. The financial support from COSMOS and U. S. Geological Survey is also gratefully acknowledged.

Contents

Effects of Strong-Motion Processing Procedures on Time Histories, Elastic, and Inelastic Spectra: Final Report

P. BAZZURRO
B. SJOBERG
N. LUCO
W. SILVA
R. DARRAGH

ABSTRACT

This article presents a statistical study on the influence of various signal-processing techniques used for filtering ground motion records on both elastic and inelastic response spectra. Consideration is also given to the effects of the filtering techniques on the resulting accelerograms. In this study we consider only the use of Butterworth filters on both real and synthetic records for near-source conditions. Other filters, such as the Ormsby filter and the elliptical filter, are also used for ground motion signal processing but are less common. While results of this study are most directly relevant to the engineering community, they also provide insight for seismologists who generate processed records for engineering applications into the practical effect of their processing techniques. As such, this information could potentially be useful to seismologists in evaluating the relative merits of different filtering methods used on records provided to one of their largest user groups. For a suite of real records we performed a sensitivity analysis to quantify the effects of the following:

- causality of the filter
- filter order
- high-pass corner frequency value
- preservation of the residual static displacement in a record

In the case of synthetic records, the differences in elastic and inelastic spectra that arise from applying a causal filter versus an acausal filter versus no filter at all were also investigated. Among the acausal filters, we considered as base cases both the 4-pole filter used by the California Strong Motion Instrumentation Program and the "cascade" 2-pole/2-pole filter that imitates the technique used by U.S. Geological Survey. Statistical results indicate that both causal filters and cascade acausal filters seem to produce spectra that are more sensitive to the selection of the filter parameters than "non-cascade" acausal filters. In general, for all filters, (a) the spectra tend to be more sensitive to the filter characteristics in the longer period range of the spectrum (i.e., closer to the high-pass corner frequency); and (b) inelastic spectra are more sensitive than elastic spectra. Among the parameter variations considered here, removal or preservation of the residual static displacement has the largest impact on both the resulting accelerograms and on the elastic and inelastic

spectra. Systematically different spectra are also observed when the value of the high-pass corner frequency is changed. The difference is noticeable at oscillator periods much shorter than the reciprocal of the high-pass corner frequency, especially for very severe levels of inelastic response, due to the effective period lengthening that occurs when oscillators behave inelastically. Among the ground motion parameters that we monitored, only peak ground displacement and, to a lesser degree, peak ground velocity were affected by the filter selection. Peak ground acceleration, Arias intensity, and duration were found to be relatively stable.

INTRODUCTION AND MOTIVATION

For structural engineers in seismic regions, the relationship between earthquake ground motion and structural performance is of primary concern for the design of new structures, the evaluation of existing ones, and the estimation of potential earthquake-induced losses to single buildings or a portfolio of properties. Modern nonlinear structural dynamic analysis software allows engineers to realistically estimate the building response and consequent damage resulting from an earthquake through time-history analysis of the ground motion acceleration record (i.e., accelerogram). Time-history analysis entails applying the record to the base of a computer model of the structure and computing the time-step by time-step response of the structure from the differential equation of motion. The "raw" ground motion signals that are recorded from an earthquake are always pre-"processed" by seismologists at major organizations such as the U.S. Geological Survey (USGS), the Pacific Earthquake Engineering Research Center (PEER), and the California Strong Motion Instrumentation Program (CSMIP) before being made available for engineering and seismological analysis. Each of these organizations uses different signal processing techniques to process their records.

It has long been known that different signal processing techniques affect the resulting ground motion time history in different ways. For example, the velocity-pulse shape and the long-period content of the processed accelerograms can be particularly sensitive to the processing technique. Moreover, causal filtering alters the phase spectrum of the time history to preserve causality (maintain the correct arrival time for each frequency component) but results in a sensitivity of motions to the filter corner frequency at frequencies much higher than the high-pass corner frequency [1]. Acausal filtering leaves the phase spectrum unaltered but results in spurious pre-event low frequency transients in the time history. Additionally, acausal filtering requires significantly larger quiet periods (zero motion) added to the recording prior to filtering to accommodate the longer filter transient. These transients are retained in the baseline corrections and integrations to velocity and displacement produced by the data providers. The time histories are then truncated to their original lengths resulting in an inconsistency between integrations of the truncated acceleration time history and the integrations provided by the processing agency. To preserve consistency, the entire acceleration time history, including processing transients, must be supplied by the data provider and used in structural analyses. Causal filtering eliminates this inconsistency but results in a dependence of high frequency motions on the corner frequency of the high-pass filter. Processing of strong-motion recordings is largely an assessment of tradeoffs in terms of potential undesirable effects and their impacts on downstream analyses. Given these premises, it is intuitive to expect that the response of structures, whether linear or nonlinear, may be affected to some degree by the different characteristics of the input signal due to different filtering techniques.

Recently Boore and Akkar [1] showed for a limited set of records, which were processed with both causal and acausal versions of a Butterworth filter with different corner frequencies, that the linear and, more significantly, the nonlinear response of oscillators can be indeed significantly affected. The difference in peak

response was up to almost 100% for some oscillator periods. Those results, however, were based on a limited set of records. Additionally, both Boore [2] and Gregor et al. [3] have shown that different processing procedures for retaining static displacements can have a large effect (i.e., 10-30%) on the response at high frequencies. To be more useful to the engineering community, the effect of various filter parameters and techniques on the linear and nonlinear response of structures of different vibration periods and yield strengths should be quantified on a *statistical* basis for a larger pool of records processed with different techniques.

The lack of quantification of systematic differences in ground motion time histories (acceleration, velocity, and displacement), and linear and nonlinear structural responses introduced by various processing techniques may have potentially serious effects in real-life engineering applications. Users of processed records need to be aware if two processing procedures generate ground motion records that cause *systematically* different responses for structures of given characteristics. For example, if the first procedure can be considered as a benchmark, then a systematic difference in structural response introduced by the second approach can be thought of as a bias. In other words, the records generated from the second approach can be considered, on average, to be either *too benign* or *too severe*. If that is the case then, engineers need to be aware of the bias and perhaps account for it in their calculations. Failure to do so may generate potentially ill-designed structures or inaccurate structural damage and loss estimates. Seismologists, who generate processed records for engineering applications, should also be interested in understanding the possible systematic differences in structural responses introduced by different processing techniques. This information could potentially be useful in evaluating the relative merits of different processing methods.

Which processing technique yields unbiased structural responses is, of course, unknown. In an attempt to shed some light on this issue, we have also considered a set of simulated records, as we will see in the next section. The unfiltered version of these simulated records could be construed as being the "true," noiseless signal. Therefore, the structural response to this noiseless suite of signals could be considered as the benchmark that is missing when dealing with real records.

The issue of potential systematic differences in structural response due to the choice of ground motion signal processing technique may have a ripple effect beyond the time-history analysis of structures. Empirical attenuation relations for peak ground motion parameters [e.g., peak ground acceleration (PGA), peak ground velocity (PGV), and peak ground displacement (PGD)] as well as elastic and, more recently, inelastic spectral quantities, rely on signal processing techniques to produce accurate representations of free-field motions. Additionally, numerical ground motion simulation procedures generally develop distributions for model parameters based on fits or comparisons to recorded (processed) data.

The key question addressed in this study is how significant the variation in the linear and nonlinear response of different structures is to the same ground motion records processed with different filtering techniques. In line with the prevalent engineering perspective of this study, the structural response is characterized here via linear elastic and nonlinear response spectra of single-degree-of-freedom (SDOF) oscillators, rather than, for example, Fourier spectra. In addition, differences in the processed time histories will be investigated. The results of this study are intended to provide a quantitative basis for:

- The engineering and seismology communities, who are the end users of ground motion records, for consideration during their applications.

- The ground motion processing organizations for facilitating discussions on future processing standards of records for engineering and seismological analyses.

Finally, we emphasize that the results presented in this study are generally based on common filtering practice and on the filter parameter values (e.g., corner frequencies) used in current applications for typical strong-motion records. These results may not be directly applicable either to other filtering techniques or to the same techniques investigated here but with different parameter values (e.g., corner frequencies).

EARTHQUAKE RECORD DATABASE AND PROCESSING TECHNIQUES

Before addressing the description of the earthquake database and the filters applied the accelerograms, we emphasize to the reader that in this section and throughout this article we tend to use terminology that pertains to the time domain (e.g., oscillator period) when the discussion is more relevant to engineers. Conversely, we use frequency-domain language when the topic is more germane to seismologists. Therefore, both oscillator period and its reciprocal, oscillator frequency, are used in what follows.

The earthquake ground motion database used in this study mainly includes real and synthetic near-source *filtered* records. As anticipated in the previous section, synthetic *unfiltered* ground motions are considered because the responses obtained using such signals can be used as a benchmark for evaluating the responses generated by the filtered synthetic record datasets.

The database of real records, listed in Table 1, comprises both strike-parallel and strike-normal horizontal components from seven earthquakes (four strike-slip and three dip-slip rupture mechanisms) ranging in magnitude from 6.5 to 7.6. The events were recorded at twenty stations on different types of soil with a source-to-site distance that ranged from 0.2 km to 17 km. In addition to these twenty pairs, a single parallel component record from the Kocaeli earthquake, which was recorded at the Sakarya station, was included in the analyses. The Sakarya normal component was not available because of failure of the accelerograph. This set of real records contains accelerograms with a fault rupture directivity parameter, $X\cos\theta$ or $Y\cos\phi$ [4], ranging from essentially zero (i.e., backward directivity region) to almost unity (i.e., strong forward directivity region) for which the most pulsive ground motion recordings are expected. Recall that for strike-slip events, X is the fraction of the fault rupture length between the epicenter and the site, and θ is the angle between the fault strike and the direction from the epicenter to the site. For dip-slip events, Y is the fraction of fault rupture width between the hypocenter and the site, and ϕ is the angle between the fault dip and the hypocentral direction to the site. Note that the last column of Table 1 reports the directivity modification factor (DMF) [4], which is the factor that the median (i.e., the geometric mean) horizontal spectral acceleration is multiplied by to account for near-source directivity effects. This factor increases with oscillator period. The range of DMF values in Table 1, which applies to periods greater than or equal to 0.75 sec for strike-slip events and greater than or equal to 1.0 sec for other mechanisms, helps discriminate between forward directivity (DMF>1) and backward directivity (0<DMF<1) records.

To assess the effects of various processing procedures on acceleration, velocity, and displacement time histories, and on linear and nonlinear structural response spectra, the 41 real records (two components for each of the 20 stations and the additional parallel component at the Sakarya station) were processed using different techniques and different parameter values for each technique. A Butterworth filter was used in all cases. Drs. Walter Silva and Robert Darragh of Pacific Engineering and Analysis (PEA) selected

Table 1. List of the twenty near-source pairs of normal and parallel components from seven earthquakes that were used in this study. In addition, we used the parallel component recorded at Sakarya for the Kocaeli earthquake. This 21st record was used in the statistics for parallel records. (Legend: S = strike-slip; R = reverse; N = normal; P = parallel). Vs30 is the average shear wave velocity to a depth of 30 m. Xcosq and Ycosf are the fault rupture directivity parameters used by Somerville et al. [4]. DMF is the directivity modification factor from that reference that multiplies the median spectral acceleration (at periods above 0.75 sec for strike-slip events and above 1.0 sec for other mechanisms) to obtain the median spectral acceleration at a near-source site.

Earthquake	Year	Mag	Rupture Mechanism	Distance (km)	Station Name	Vs30 (m/s)	Comp.	HP (Hz)	LP (Hz)	Xcos(q) or Ycos(ϕ)	DMF
Imperial Valley	1979	6.5	S	8.5	Brawley Airport	209	N	0.10	40	0.7	1.05-1.54
							P	0.10	40	0.7	
				1	El Centro Array #6	203	N	0.10	40	0.5	1.00-1.08
							P	0.10	40	0.5	
				0.6	El Centro Array #7	211	N	0.10	40	0.5	1.00-1.08
							P	0.10	40	0.5	
				14.2	Parachute Test Site	349	N	0.10	40	0.7	1.05-1.54
							P	0.10	40	0.7	
Loma Prieta	1989	6.9	R (oblique)	6.1	LGPC	466	N	0.10		0.8	1.04-1.17
							P	0.10		0.8	
Landers	1992	7.3	S	1.1	Lucerne	685	P	0.08	60	0.63	1.03-1.36
							N	0.08	60	0.63	
Kobe	1995	6.9	S	10.2	Amagasaki	256	P	0.10	40	0.57	1.02-.123
							N	0.10	40	0.57	
				0.2	Kobe University	1043	P	0.10	30	0.42	0.94-0.99
							N	0.10	30	0.42	
				2.5	Port Island (0 m)	198	P	0.10		0.3	0.76-0.97
							N	0.10		0.3	
				1.2	Takarazuka	312	P	0.13	33	0.64	1.03-1.39
							N	0.13	33	0.64	
Northridge	1994	6.7	R	6.2	Jensen Filter Plant	373	P	0.20		0.79	1.04-1.16
							N	0.20		0.79	
				7.1	Rinaldi Receiving Stn.	282	P	0.10		0.77	1.03-1.15
							N	0.10		0.77	
Kocaeli, Turkey	1999	7.4	S	17	Arcelik	523	N	0.07	50	0.26	0.71-0.96
							P	0.07	50	0.26	
				12.7	Duzce	276	N	0.08	15	0.51	1.10-1.10
							P	0.08	15	0.51	
				17	Gebze	792	N	0.08	25	0.23	0.68-0.96
							P	0.08	25	0.23	
				4.8	Izmit	811	P	0.10	30	0.02	0.46-0.92
							N	0.10	30	0.02	
				2.6	Yarimca	297	N	0.07	50	0.11	0.55-0.94
							P	0.07	50	0.11	
				3.1	Sakarya	471	P	0.04	40	0.19	0.63-0.95
Chi-Chi, Taiwan	1999	7.6	R	4.4	TCU049	N/A	P	0.02	30	0.62	1.00-1.03
							N	0.02	30	0.62	
				0.2	TCU052	N/A	P	0.04	50	0.61	1.00-1.02
							N	0.04	50	0.61	
				1.1	TCU068	N/A	P	0.03	50	0.62	1.00-1.03
							N	0.03	50	0.62	

Table 2. List of record subsets that were processed by each filtering technique. (Legend: N = normal component, P = parallel component). The 21st parallel component record associated with many of the subsets is the Kocaeli (Sakarya) record. The records in Row 10 are original records processed by CSMIP and were used only to check the consistency of PEA's and CSMIP's acausal filtering techniques.

Row #	Filtering Technique	Records Filtered
1	Cascade Acausal (2-pole/2-pole)	All real records (20 N, 21 P)
2	Cascade Acausal (2-pole/2-pole, 1.5 x HP)	All real records (20 N, 21 P)
3	Cascade Acausal (2-pole/3-pole)	All real records (20 N, 21 P)
4	Acausal (4-pole)	All real records (20 N, 21 P)
5	Acausal (4-pole, 1.5 x HP)	All real records (20 N, 21 P)
6	Causal (4-pole)	All real records (20 N, 21 P)
7	Causal (4-pole, 1.5 x HP)	All real records (20 N, 21 P)
8	Acausal (5-pole)	All real records (20 N, 21 P)
9	Causal (5-pole)	All real records (20 N, 21 P)
10	CSMIP Acausal	Chi-Chi (TCU049, TCU052, TCU068) (3 N, 3 P)
11	Static	Chi-Chi (TCU049, TCU052, TCU068) (3 N, 3 P) Landers (Lucerne) (1 N, 1 P) Kocaeli (Izmit, Yarimca, Sakarya) (2 N, 3 P)
12	Acausal (5-pole)	30 average horizontal ground motion realizations of M7.1 event on Hayward Fault (5 km source-to-site distance). Earthquake nucleation point and fault slip were varied in each realization. High-pass and low-pass corner frequencies were 0.1Hz and 50Hz, respectively.
13	Causal (5-pole)	Same as Row 12.
14	No Filter	Same as Row 12.

the records, rotated them to obtain fault-parallel and fault-normal components, and performed the signal processing. The filters were applied in the frequency domain in all cases. Records were not processed with an Ormsby filter because at the time of this writing that processing technique is no longer used by CSMIP with the exception of accelerograms recorded on older analog instruments. Given that other organizations such as the University of Southern California still use the Ormsby filter, we suggest that it and others (e.g., the elliptical filters used by Imperial College, London) be included in a future expansion of this comparative study.

The cases that were considered are listed in Table 2 and are identified by a *row number* to facilitate inspection of the results in the figures to come. Note that when in the rest of the report a row number is quoted, we often drop the reference to Table 2 for conciseness. Also, when a notation such as Row *i*/Row *j* in conjunction with ratios of response spectra is used, we mean that the ratios are generated by dividing the spectra produced by input data in Row *i* by the corresponding spectra produced by input data in *Row j*.

In particular, the following low-pass/high-pass filter pairs were considered:

- causal Butterworth 4-pole filter currently used by PEER (Row 6)

- "cascade"[1] acausal Butterworth 2-pole/2-pole filter to emulate[2] current USGS processing (Row 1)
- acausal Butterworth 4-pole filter currently used by CSMIP (Row 4)

To facilitate the understanding of the effect of filter order on the shape of the frequency response function, Figure 1 shows the gain function (in decibels) plotted versus frequency (normalized by the corner frequency, f_c) for four filters used in this study.

The available values of the high-pass (HP) and low-pass (LP) corner frequencies used for the base case analysis of records in this study are reported in Table 1. Besides investigating the effect of filter causality on oscillator response, the filter order and corner frequencies were also varied on all three base case versions of the Butterworth filter listed previously. To be precise, a causal 5-pole (Row 9), a cascade acausal 2-pole/3-pole[3] (Row 3), and an acausal 5-pole (Row 8) were used to process the raw records. To vary the HP frequency corner, the values reported in Table 1 were multiplied by a factor of 1.5 (e.g., 0.15 Hz instead of 0.10 Hz for the Brawley Airport record of the Imperial Valley earthquake). The 4-pole causal case with HP corner frequency multiplied by 1.5 is in Row 7, the cascade 2-pole/2-pole acausal with HP corner frequency multiplied by 1.5 is in Row 2, and the acausal 4-pole case with HP corner frequency multiplied by 1.5 is in Row 5. The LP frequency corner was not varied because it is well outside the structural period range of interest in this study and therefore has no effect on structural response.

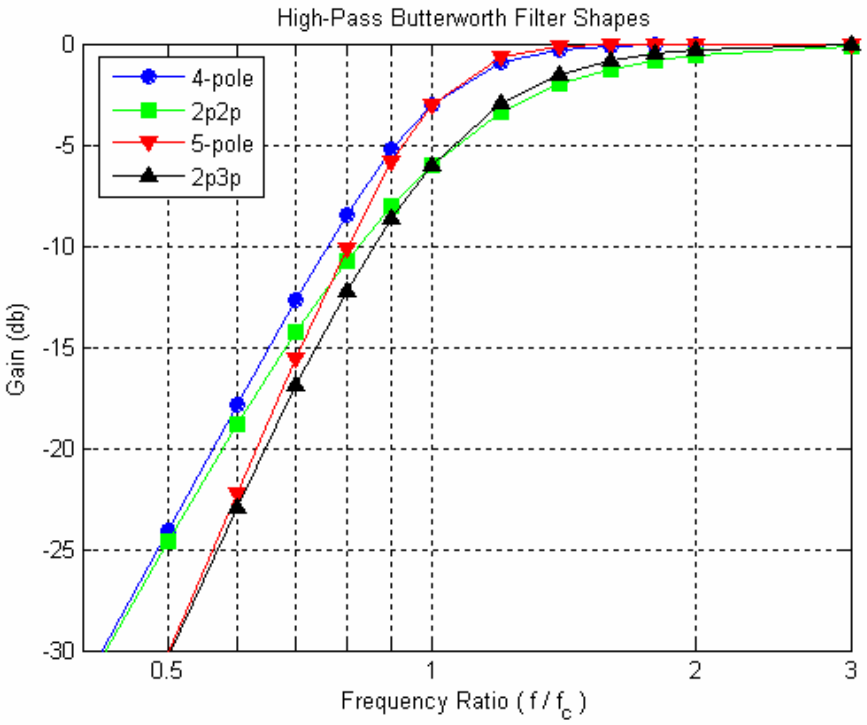

Figure 1. Frequency response of Butterworth filters of different order.

[1] A "cascade" filter refers to two filters (e.g., 2-pole and 2-pole) that are applied sequentially in the frequency domain.
[2] USGS applies acausal filtering in the time domain. Dr. Boore of USGS has applied the USGS technique to a subset of records and the resulting spectra are indistinguishable from those used in this study.
[3] Two-pole filtering followed by 3-pole filtering, both applied in the frequency domain.

To evaluate the effect of static displacement on oscillator response, an approach for preserving static displacements [3] [5] [6] was applied to records from six of the twenty stations (see Table 1 and Table 2). This approach involves only baseline correcting and low-pass filtering each record. This case is labeled "Static" in Table 2 (Row 11) and thereafter in this document.

The last set of real records used in this study is listed in Row 10 of Table 2. These records, unlike all others, were processed by CSMIP rather than PEA. This subset of records was only employed here to confirm that the CSMIP acausal filtering technique emulated by PEA (Row 4) produced similar linear and nonlinear responses as the records processed directly by CSMIP. The spectra for the records included in both Row 10 and Row 4 were essentially indistinguishable. For conciseness, no results are shown here.

The synthetic ground motion dataset used in this study consisted of 30 realizations of the average horizontal component, based on the root-mean-square (RMS) of the Fourier amplitude spectra of the two horizontal components. The RMS average, compared to a geometric average, is invariant under component rotation, relaxing the necessity to rotate components to random orientations at each realization. This avoids a potential bias in the site response control motions if a geometric average were used with components held at fixed orientations. The simulation methodology uses the stochastic finite fault approach, which employs random vibration theory equivalent-linear site response analyses to approximate nonlinear soil effects [7]. This method has been validated with geometric average horizontal component response spectra computed from motions of 15 earthquakes recorded at about 500 sites [7]. For this project, site conditions reflect soft soils (i.e., bay mud; for details see Silva et al.[8] [9]) with the site located at a five-kilometer rupture distance from a **M** 7.1 earthquake on the Hayward fault. In the randomization process, site dynamic material properties (shear-wave velocity, layer thickness, shear modulus ratio G/Gmax and hysteretic damping curves) as well as slip model and nucleation point were varied using empirical distributions [7]. Given that the location of the earthquake nucleation point was randomized, the site did not always lie in the forward directivity region. This set of 30 records was processed using both a 5-pole acausal filter (Row 12) and a 5-pole causal filter (Row 13). As mentioned earlier, the same synthetic records were left unprocessed (Row 14) to determine the benchmark oscillator response.

DESCRIPTION OF THE RESPONSE ANALYSES

The pool of real and simulated records described previously was used to perform dynamic analyses of linear and nonlinear 5%-damped SDOF oscillators with periods ranging from 0.1 sec to 10 sec (or alternatively, in frequency terms, from 10 Hz to 0.1 Hz). Time-history analysis of each record was performed using a suite of oscillators (again, either linear or nonlinear) and the absolute value of the peak-in-time response (e.g., the horizontal displacement of the mass) of each oscillator is noted down. Figure 2 shows the peak displacement value, D_{max}, of both a linear and a nonlinear 1 sec oscillator subjected to the ground motion accelerogram in the top panel. A response spectrum of a given record for the desired response measure is simply the locus of the peak values reached by all the oscillators of different vibration period. The backbone force-deformation curve (see Figure 2 for a schematic description of the loading portion of it) of the nonlinear oscillators is bilinear with 2% post-yield hardening (called a in Figure 2) and a hysteretic rule that has no degradation of either strength or stiffness and the same loading and unloading slope. The response measure chosen here for statistical analysis is the same peak horizontal displacement, D_{max}, mentioned above, which hereafter will be called S_d (for spectral displacement) for historical reasons.

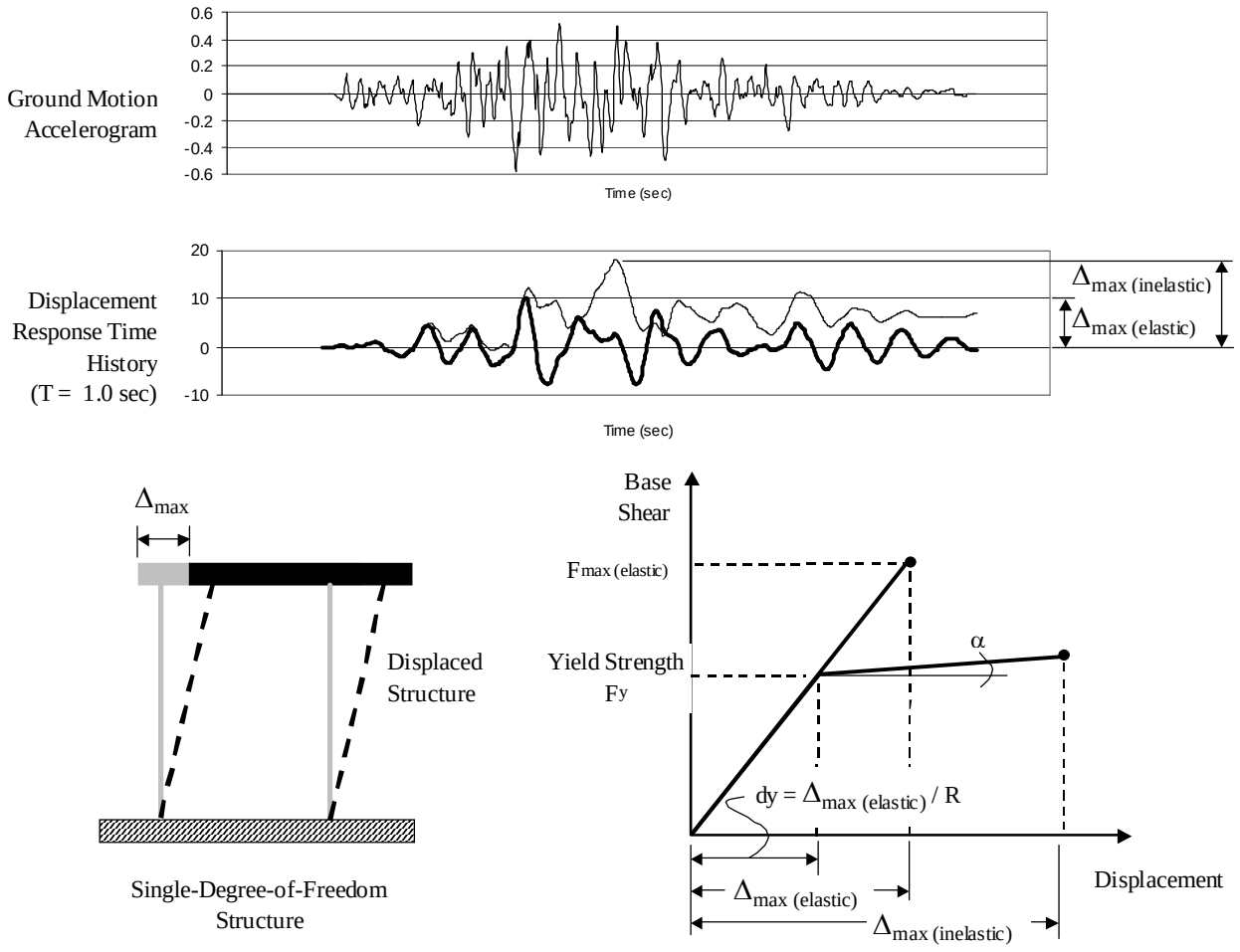

Figure 2. Schematic of SDOF structure and yield strength definition. The quantity a is the post-yield hardening here set equal to 2%. The yield strength in the figure is called F_y in the text.

To ensure a response that ranges from mildly inelastic to severely inelastic, three "strength" levels for the SDOF system at each oscillator period were selected. The elastic response case was also included in this study both for completeness and for checking purposes. The nominal strength levels of the nonlinear SDOF oscillators were set as a fraction equal to 1/R of the peak elastic base shear, F_{max}, where R³1, that is $F_y=F_{max}/R$, (R=1 being the elastic case), as shown in the bottom panel of Figure 2. Equivalently, the yield "strength" of the nonlinear oscillator can be set in displacement terms as $d_y=d_{max}/R$, as shown again in the bottom right panel of Figure 2. This procedure follows a common seismic design practice. Loosely speaking, structures are designed to remain elastic when they experience a base-shear force induced by an earthquake ground shaking that is R times smaller than the value induced by a target design motion. The target design motion in modern codes is often selected to be equal to the level expected at the site for a given mean return period (e.g., 475 years or 10% exceedance probability in 50 years). The "appropriate" value of R for a given building type (e.g., steel moment-resisting frame) is chosen according to the level of post-elastic deformation that the structural system is expected to withstand without collapsing.

The three strength levels selected in this study are characterized by R values equal to two (mildly inelastic), four, and eight (severely inelastic). The results for R=2 were computed but not shown as they are closely bracketed by the results for the elastic case and the R=4 case. Note that the level of nonlinear responses imply, for some SDOF systems, very large ductility values that, of course, may not be physically attainable by all real structures. It should be understood, however, that the peak value of the elastic base shear, or equivalently the peak elastic deformation, experienced by an elastic structure is a ground-motion-specific quantity. Therefore, one can achieve the same value of R either: (a) for *each record* in a dataset; or (b) in an *average sense for all the records* in the same dataset. In the former case an uniform target R value can be attained by varying the yield displacement of the structure, d_y, from record to record. More precisely, for each record d_y is set equal to the peak elastic displacement for that record divided by the desired value of R (see Figure 2). It should be emphasized that according to this procedure an SDOF system with a given natural period has different strength characteristics for each ground motion record.

Usable Bandwidth

As noted above, SDOF systems with natural frequencies that ranged from 0.1 Hz to 10 Hz were used in this study. Two records in Table 1 were processed using a high-pass (HP) frequency of 0.20 Hz while all others were processed with HP frequencies of 0.1 Hz or lower. While the natural frequency value of 10Hz is well below the individual LP corner frequency, f_{LP}, used for signal processing of each record, the value of 0.1 Hz is in the neighborhood of the HP corner frequencies, f_{HP}, used for processing some of the real records. This may potentially generate some concerns regarding the accuracy of the low-frequency part of the response spectra (especially the nonlinear ones).

Ideally, the usable bandwidth should be set in such a way that no significant signal has been filtered out within the defined frequency band. Therefore, usually the recommended usable bandwidth of records is narrower than the range bound by the corner frequencies and depends on the characteristics of the filter adopted. For example, the cascade acausal 2-pole/2-pole Butterworth filter used by USGS decays more slowly outside of the corner frequencies than both the 4-pole acausal filter used by CSMIP and the 4-pole causal filter used by PEER, but it has a larger attenuation within a multiplicative factor of two on either side of the corner frequency (Figure 1). In other words, the frequency response function of the 2-pole/2-pole filter in the range of f/f_c from 0.5 to 2 is lower than the frequency response functions of the 4-pole causal and acausal filters. This translates into a narrower usable bandwidth for the USGS filter as compared to that for the filters used by CSMIP and PEER.

Consequently, it should not come as a surprise that each of the three organizations provides different specifications on the usable bandwidth issue for its own processed records. PEER recommends considering SDOF systems with a fundamental frequency ranging between f_l and f_h where $f_l = f_{HP} \times 1.25$ and $f_h = f_{LP} / 1.25$. USGS recommends using a factor of two instead of 1.25 and CSMIP recommends a factor of 1.0. The upper and lower bounds of the recommended usable bandwidth for each filter type are shown by vertical lines in the figures that display the response spectra results in the following sections. Note that the lines were drawn for the *most restrictive* case out of all the records included in the dataset. Hence portions of the results drawn outside the usable bandwidth indicated in the figures to come are generated from records whose majority may still be within their individual usable ranges. For example, the long-period (upper) bound of the usable bandwidth in the *least restrictive* record is about ten times that shown in the figures. Hence, as a first approximation, we can conclude that the statistical validity of the results holds, to some extent, even outside the restrictive bands drawn in the figures to come. Note also that the figures to come

present the results in the time domain and not in the frequency domain. Therefore, to delimit the usable bandwidth we use the quantities $T_c = 1/f_{HP}$ and $T_{c(LP)} = 1/f_{LP}$.

As a final comment on the usable bandwidth, it is emphasized that the recommended bounds reported above were set with no specific attention to the use of such records as input to structural *nonlinear* dynamic analyses. The effective structural period of vibration may significantly lengthen outside the suggested usable bandwidth of the record as the damage severity progresses. Therefore the usable lower frequency will tend to be somewhat higher (more restrictive) for such cases. In this study we have not made any attempt to revisit the adequacy of such recommendations under this light. This topic deserves further research.

Response Spectra and Fourier Spectra

The results in this study are presented in response spectra terms that are most familiar to engineers. Note, however, that the *linear elastic* response spectrum of a linear *narrow-band* oscillator behaves very similarly (especially for undamped oscillators) to the Fourier amplitude spectrum of the *broad-band* input signal, which in turn is directly impacted by the shape of the filters used by the processing technique. Therefore, qualitatively speaking, the ratios of the linear elastic response spectra obtained from the different techniques that are presented later in this study are expected to look somewhat like the ratio of filter shapes.

This study also considered nonlinear spectra of three sets of oscillators with different strength values described by the values of R equal to two, four and eight. The response of these oscillators tends to be very nonlinear especially for the oscillators with lower yield strength (i.e., higher R value). The response of these highly nonlinear oscillators is not so narrow banded as in the linear case because it is also very sensitive to the input at periods longer than the natural period. This is due to the lengthening of the period as damage grows. Therefore, the relationship between the Fourier spectrum of the input record and the response spectrum of the nonlinear oscillator is less direct.

RESULTS

Sensitivity Analysis: Causal versus Acausal Butterworth Filters

To investigate this issue, the response results for records processed using a 4-pole causal filter (Row 6), a 4-pole acausal filter (Row 4), and a cascade 2-pole/2-pole acausal filter (Row 1) were compared. Normal and parallel components were analyzed separately to check for differences in the results.

Table 3 (*Panel a)* summarizes the median (i.e., the geometric mean) of the ratio of global ground motion parameters, such as PGA, PGV, PGD, Arias intensity (AI), and bracketed 5%-95% energy-based Trifunac duration (T_D) obtained from the records processed by the three aforementioned techniques. Statistics of the ratio of the elastic and inelastic displacement response spectra for different values of R are shown in Figure 3 and summarized in Table 3 (*Panels b* and *c*). Note that the standard deviation, σ, is computed in natural logarithm terms and, therefore, is numerically close to the coefficient of variation (for values less than about 0.3). From an inspection of the results for *linear elastic* (i.e., R=1) SDOF systems (*Panel a* in Figure 3) and from results in *Panel a* of Table 3 it is clear that:

- PGD and, to a lesser extent, PGV are affected by the causality of the filter while PGA, AI, and T_D are not. In particular, the median values of PGD and PGV for the acausal filter appear to be systematically higher than the medians from both the causal filter and the cascade acausal filter of the same order.

- The ratio of the spectra obtained from causal and acausal filters is, on average, nearly one (i.e., the median curve is around one across the entire frequency range).
- The ratio of the spectra obtained using two versions of acausal filters is very close to one up to the upper bound of the usable bandwidth of the filters. At longer periods, the larger attenuation of the cascade acausal filter causes the spectrum ratio to increase (Figure 3, *Panel a*, right).
- There is record-to-record variability in the linear spectrum ratios but the discrepancies do not seem to systematically appear at specific frequencies. The variability tends to increase with oscillator period.
- As expected, the variability in the ratio of spectra found using causal and acausal filters (Figure 3, *Panel a*, left) is larger than the variability in spectra obtained using two different versions of acausal filters (*Panel a*, right).

The results of the *nonlinear* analyses presented in Figure 3 for R=4 (*Panel b*) and R=8 (*Panel c*) confirm the same conclusions itemized above. However, the record-to-record variability is considerably larger in the nonlinear domain (σ up to 0.2 to 0.3 at some periods for the causal/acausal case and up to 0.1 to 0.2 for the acausal/acausal case). The limited sample size and this relatively large variability prevents us from stating that the inelastic spectra generated by records filtered using a causal procedure are systematically lower than those produced using an acausal filter. This trend, however, is suggested by the median curve of the ratio being consistently below one at almost all periods for both R=4 (*Panel b*) and R=8 (*Panel c*). A two-sided *t-test* shows that the difference in the ratio from unity is statistically significant at a 10% level at only a few periods in the neighborhood of 1.0 sec. In the case of the two versions of the acausal filters, the inelastic spectra are, on average, indistinguishable (within the usable bandwidth). Note that the median $\pm \sigma$ curves in Figure 2 (and in all the other that follow) represent approximately the 84%-ile and the 16%-ile curves of the ratio of the spectra (i.e., they are found by multiplying the median curves by $\pm \exp(\sigma)$, where σ is the standard deviation of the natural logarithm of the spectrum ratios).

Note that although Figure 3 was derived from processing the normal components of the ground motions, similar conclusions can be drawn from the results obtained separately for the parallel components. A comparison of R=4 (Normal) and R=4 (Parallel) in Table 3 (*Panel c*) shows similar trends in the normal and parallel record response results.

Sensitivity Analysis: Filter Order

The effects of filter order on peak ground motion parameters and on elastic and inelastic spectra were studied for the three versions of the Butterworth filters considered here, namely a causal filter (Row 6 and Row 9), an acausal filter (Row 4 and Row 8), and a cascade acausal filter (Row 1 and Row 3). Only filters of order four and five were considered in this sensitivity analysis.

The differences in the values of ground motion parameters induced by the filter order are presented in Table 4 (*Panel a*), while the differences in elastic and inelastic spectra are shown in Figures 4a, 4b, and 4c and summarized in Table 4 (*Panels b* and *c*) for the three cases above. Table 4 (*Panel b*) presents statistics of the ratio of the displacement response spectra averaged across frequencies (within the boundaries of the suggested bandwidth). As before, most of the results shown (for R=1, 4, and 8) were generated using normal components

Table 3. Summary of causal vs. acausal Butterworth filters. The statistics reported in Panel b-c are averaged across frequency (within usable bandwidth only). The values in Panel b bracket the statistics found for R=2 and R=4 for normal components. The standard deviation, s, is computed in natural logarithm terms and, therefore, is numerically close to the coefficient of variation (for values less than about 0.3). This table should be considered in conjunction with Figure 3.

Case	Normal					Parallel				
	PGA	PGV	PGD	Arias	T_D	PGA	PGV	PGD	Arias	T_D
4-pole Causal/Acausal	1.012	0.942	0.94	1	1	1.044	0.955	0.852	0.999	0.997
4-pole Acausal/2p2p Acausal	1.002	1.031	1.092	1.006	1	1.003	1.049	1.06	1.008	1
4-pole (x1.5 HP) Causal/Acausal	1.005	0.948	0.938	1	1.01	1.036	0.979	0.837	0.999	0.996
4-pole (x1.5 HP) Acausal/2p2p (x1.5 HP) Acausal	1.003	1.051	1.184	1.018	1	1.005	1.058	1.274	1.018	0.998
5-pole Causal/Acausal	1.008	0.931	0.92	1	1.01	1.04	0.938	0.841	0.999	0.995
5-pole Acausal/2p3p Acausal	1	1.022	1.069	1.004	1	1	1.039	1.062	1.005	0.999

(a) Median ratios of ground motion parameters

Case	R = 1 (Normal)				R = 8 (Normal)			
	Min.	Max.	Med.	σ	Min.	Max.	Med.	σ
4-pole Causal/Acausal	0.813	1.186	1.001	0.052	0.480	2.318	0.971	0.21
4-pole Acausal/2p2p Acausal	0.913	1.033	1.002	0.006	0.890	1.296	1.025	0.034
4-pole (x1.5 HP) Causal/Acausal	0.777	1.217	1.001	0.063	0.423	2.011	0.954	0.248
4-pole (x1.5 HP) Acausal/2p2p (x1.5 HP) Acausal	0.990	1.051	1.004	0.007	0.968	1.288	1.052	0.051
5-pole Causal/Acausal	0.784	1.208	1.002	0.059	0.448	2.271	0.952	0.228
5-pole Acausal/2p3p Acausal	0.995	1.019	1.002	0.003	0.935	1.175	1.018	0.022

(b) Statistics of ratios of elastic (R=1) and inelastic(R=8) response spectra for normal components

Case	R = 4 (Normal)				R = 4 (Parallel)			
	Min.	Min.	Min.	σ	Min.	Max.	Med.	σ
4-pole Causal/Acausal	0.378	2.293	0.954	0.272	0.451	2.953	0.998	0.277
4-pole Acausal/2p2p Acausal	0.840	1.216	1.014	0.031	0.669	1.835	1.022	0.057
4-pole (x1.5 HP) Causal/Acausal	0.318	2.428	0.942	0.296	0.431	3.177	0.991	0.29
4-pole (x1.5 HP) Acausal/2p2p (x1.5 HP) Acausal	0.936	1.226	1.029	0.041	0.704	1.541	1.038	0.067
5-pole Causal/Acausal	0.356	2.343	0.945	0.287	0.480	2.966	0.992	0.288
5-pole Acausal/2p3p Acausal	0.961	1.141	1.011	0.019	0.641	1.860	1.017	0.046

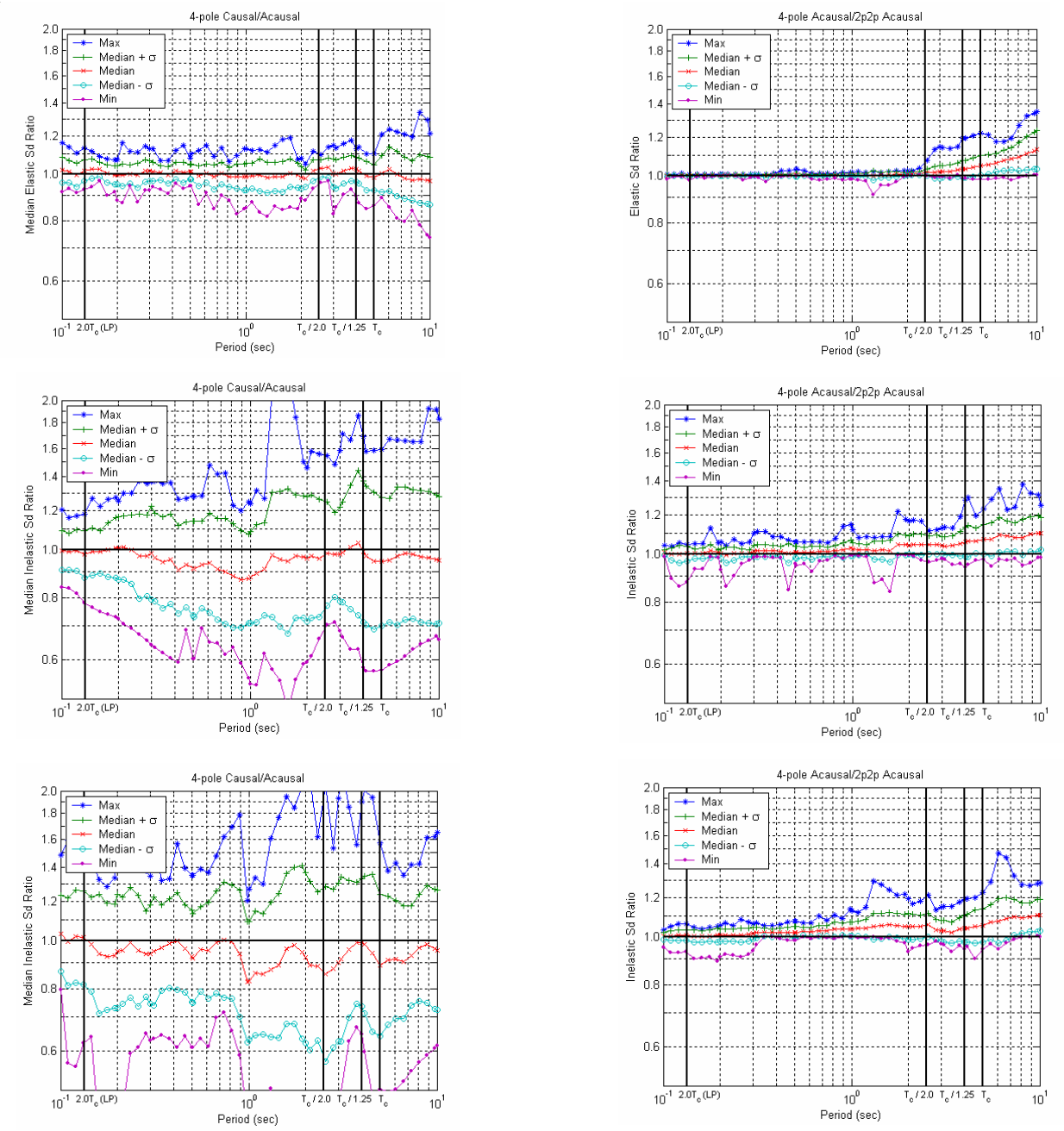

Figure 3. ***Causal vs. acausal filter comparison*: Ratio of elastic (*Panel a*) and inelastic displacement response spectra (*Panels b and c*) computed using Butterworth causal and acausal filters. The median and standard deviation, s, are computed across 20 records (normal component only). The three figures on the left were generated using spectra from data in Row 6 and Row 4 (i.e., *Row 6/Row 4*) while the three on the right were generated using spectra from data in Row 4 and Row 1 (i.e., *Row 4/Row 1*). The T_c/1.25 vertical lines are applicable for the three figures on the left, the T_c/2.0 (and $2.0T_c$(LP)) vertical lines apply to the three figures on the right, and the T_c vertical lines apply to all the figures.**

of the ground motions but a concise review of the results for parallel components (for R=4 only) is included in *Panel c* of Table 4.

Table 4 (*Panel a*) suggests that the median values of these five ground motion parameters are, for all practical purposes, not sensitive to the number of filter poles. Figure 4a through 4c show that the different filter order does not alter, on average, the elastic and inelastic spectra although record-to-record variability (increasing with period) is introduced by the change in filter order. The median ± σ curves (i.e., the 84%-ile and the 16%-ile curves of the ratio of the spectra) are jagged but the location of the peaks seems to be random. Figure 4a and 4c for the causal filter and the cascade acausal filter, respectively, show again that the variability is larger in the nonlinear domain than it is in the linear domain. The spectral ratios found by changing the order of the acausal filter (Figure 4b) are considerably more stable. No differences can be detected in the median spectral displacement response up to long oscillator periods.

Sensitivity Analysis: High-Pass Corner Frequency

The effect of increasing the HP corner frequency, f_{HP}, of the Butterworth filter for a causal 4-pole version (Row 6 and Row 7), an acausal 4-pole version (Row 4 and Row 5), and a cascade acausal 2-pole/2-pole version (Row 1 and Row 2) are presented in this section. In each case, we carried out the sensitivity analysis by multiplying the original f_{HP} value for all 20 pairs of records by a factor of 1.5.

A summary of the effect on peak ground motion parameters is given in Table 5 (*Panel a*) and the effect on elastic and inelastic displacement response spectra for the three cases listed above are reported in Figures 5a, 5b, and 5c, respectively. Table 5 (*Panels b* and *c*) presents statistics of the ratio of the displacement response spectra averaged across frequencies (within the adjusted boundaries of the suggested bandwidth). Of course, the increase in f_{HP} value decreases the usable bandwidth. For comparison purposes with normal component results, the last section of Table 5 (*Panel c*) shows the statistics for R = 4 obtained using the parallel component records.

From Table 5 (*Panel a*) it is clear that increasing the value of the high-pass corner frequency for each record by 50% affects, again, only PGD and PGV while it does not have any appreciable impact on PGA, AI, and T_d. The effect of multiplying f_{HP} by a factor of 1.5 translates into, on average, 5% lower PGV values and 15% to 20% lower PGD values regardless of whether the filter is causal or acausal.

Inspection of Figures 5a, 5b, and 5c and Table 5 shows that the main comments regarding record-to-record variability in elastic and inelastic spectrum ratios reported in the previous sections (namely, variability increasing with R, and increasing with oscillator period for the same R) still hold here. As with the filter-order comparison, the record-to-record variability of the spectrum ratio for the acausal filter is less than that for the causal and cascade acausal filters when the HP corner frequency is increased by 50%.

What is noticeably different in the f_{HP} sensitivity case is that the inelastic displacement response spectra provided by the records with the f_{HP} values reported in Table 1 are systematically higher across almost *the entire frequency range* than those generated by the same records processed with the f_{HP} values multiplied by a factor of 1.5. The median line of the ratio of spectra across the 20 stations in Figures 5a through 5c is consistently below one in all cases and more so for the severely inelastic cases (i.e., R=8) and for longer periods. A two-sided *t-test* conducted on the spectrum ratio independently at each period shows that the median spectrum ratio curve for R=8 is statistically different than one at a 10% level of significance for periods longer than approximately 1.0 sec for the 4-pole causal filter (*Panel c* of Figure 5a), 0.5 sec for the 4-

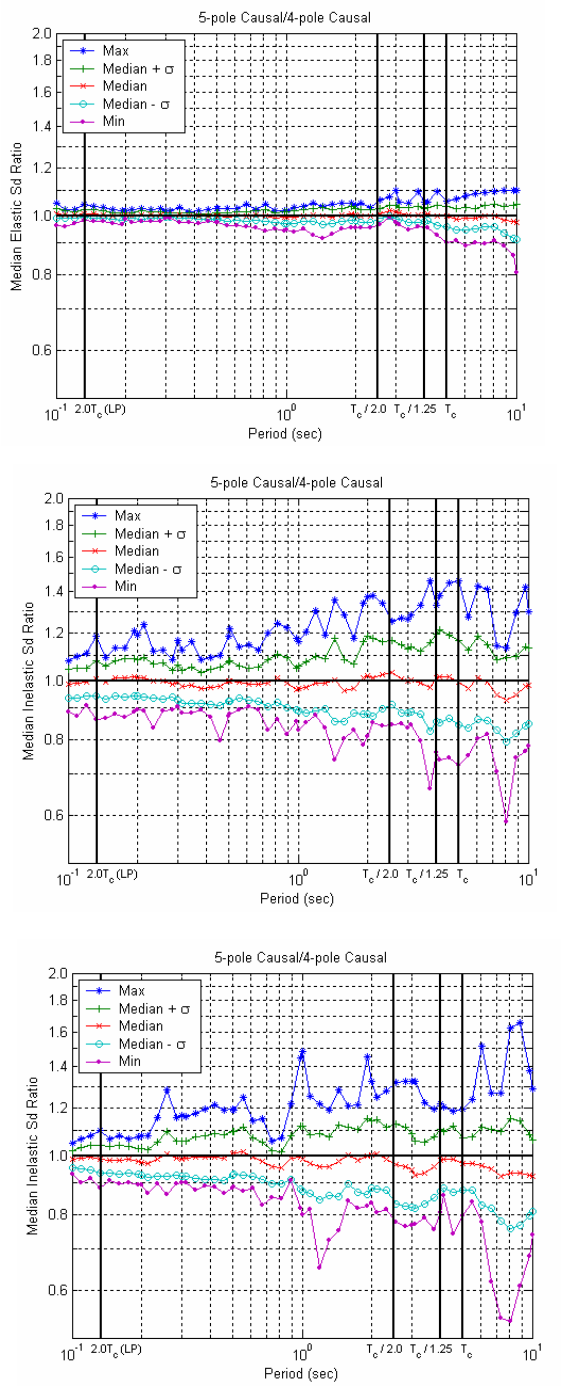

Figure 4a. ***Filter order comparison*. Ratio of elastic (*Panel a*) and inelastic displacement response spectra (*Panels b* and *c*) computed using a Butterworth causal filter with different number of poles (i.e., 5-pole/4-pole). The statistics are computed across 20 records (normal component only). The vertical line labeled T_c/1.25 is the only one relevant here. All the response spectra were created using records in Row 9 (i.e., 5-pole causal) and Row 6 (i.e., 4-pole causal) in Table 2 (i.e., *Row 9/Row 6*).**

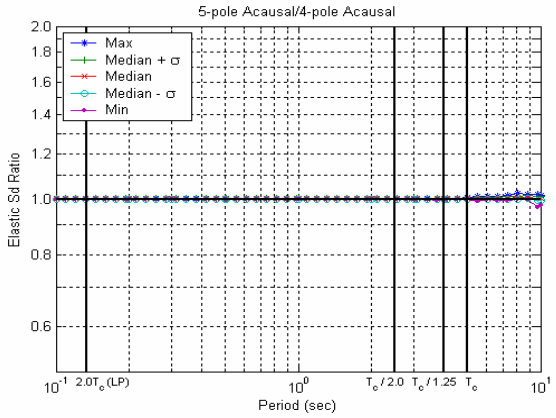

(a) R = 1 (Elastic)

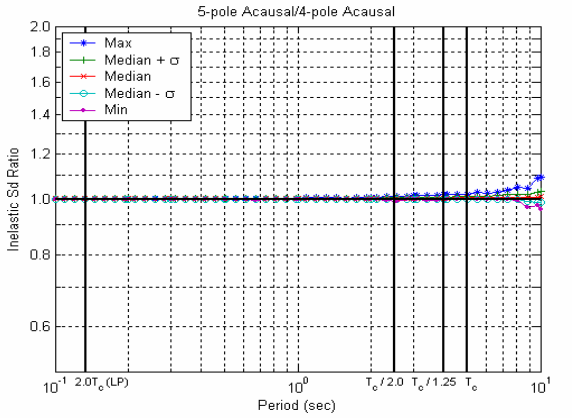

(b) R = 4

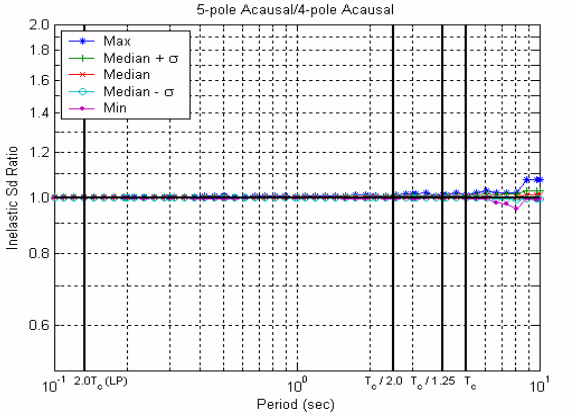

(c) R = 8

Figure 4b. ***Filter order comparison*. Ratio of elastic (*Panel a*) and inelastic displacement response spectra (*Panel b, Panel c*) computed using a Butterworth <u>acausal</u> filter with different number of poles (i.e., 5-pole/4-pole). The statistics are computed across 20 records (normal component only). The vertical line labeled T_c is the only one relevant here. All the response spectra were created using records in Row 8 (i.e., 5-pole acausal) and Row 4 (i.e., 4-pole acausal) in Table 2 (i.e., *<u>Row 8/Row 4</u>*).**

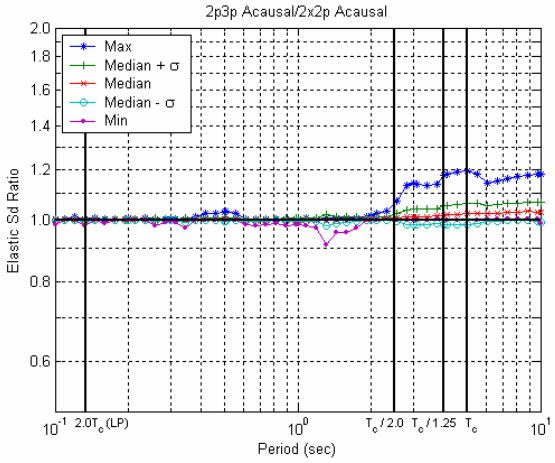

(a) R = 1 (Elastic)

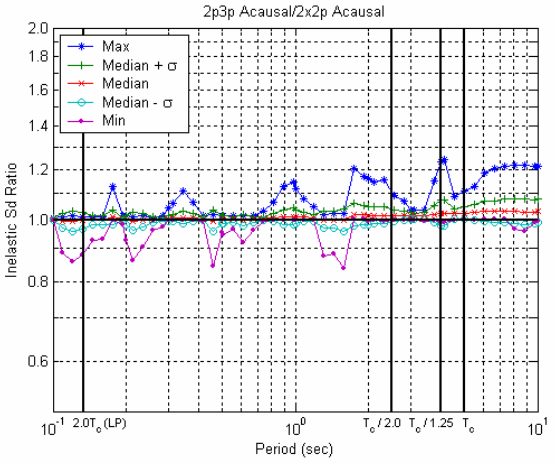

(b) R = 4

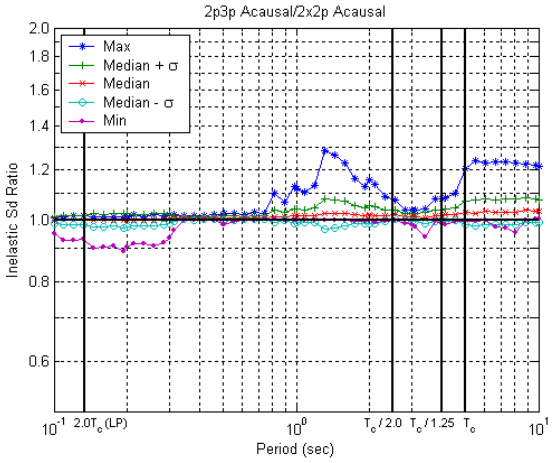

(c) R = 8

Figure 4c. ***Filter order comparison*. Ratio of elastic (*Panel a*) and inelastic displacement response spectra (*Panels b* and *c*) computed using a cascade acausal Butterworth filter with different number of poles (i.e., 5-pole/4-pole). The statistics are computed across 20 records (normal component only). The vertical lines labeled T_c/2.0 and 2.0T_c(LP) are the only ones relevant here. All the response spectra were created using records in Row 3 (i.e., 2-pole/3-pole acausal) and Row 1 (2-pole/2-pole acausal) in Table 2 (i.e., *Row 3/Row 1*).**

Table 4. Summary of *filter order sensitivity analysis*. The statistics reported in *Panels b-c* are averaged across frequency (within usable bandwidth only). The values in *Panel b* bracket the statistics found for R=2 and R=4 for normal components. The standard deviation, s, is computed in natural logarithm terms and, therefore, is numerically close to the coefficient of variation (for values less than about 0.3). This table should be inspected in conjunction with Figures 4a, 4b, and 4c.

Case	Normal					Parallel				
	PGA	PGV	PGD	Arias	T_D	PGA	PGV	PGD	Arias	T_D
5-pole Causal/4-pole Causal	0.996	0.988	0.98	1	1.01	0.995	0.983	0.986	1	0.998
5-pole Acausal/4-pole Acausal	1	1	1.001	1	1	1	1	1	1	1
2p3p Acausal/2x2p Acausal	1.002	1.009	1.022	1.002	1	1.004	1.01	0.998	1.003	1.001

(a) Median ratios of ground motion parameters

Case	R = 1 (Normal)				R = 8 (Normal)			
	Min.	Max.	Med.	σ	Min.	Max.	Med.	σ
5-pole Causal/4-pole Causal	0.918	1.102	1.001	0.018	0.652	1.487	0.982	0.089
5-pole Acausal/4-pole Acausal	0.996	1.005	1	0	0.993	1.017	1.001	0.002
2p3p Acausal/2x2p Acausal	0.914	1.03	1	0.005	0.89	1.283	1.008	0.02

(b) Statistics of ratios of elastic (R=1) and inelastic(R=8) response spectra for normal components

Case	R = 4 (Normal)				R = 4 (Parallel)			
	Min.	Max.	Med.	σ	Min.	Max.	Med.	σ
5-pole Causal/4-pole Causal	0.739	1.459	0.991	0.087	0.662	1.344	0.995	0.083
5-pole Acausal/4-pole Acausal	0.99	1.019	1.001	0.002	0.989	1.014	1.001	0.002
2p3p Acausal/2x2p Acausal	0.84	1.204	1.004	0.021	0.713	1.372	1.005	0.036

(c) Statistics of ratios of inelastic response spectra (R=4) for normal and parallel components

pole acausal filter (*Panel c* of Figure 5b), and 0.3 sec for the 2-pole/2-pole acausal filter (*Panel c* of Figure 5c). The same level of significance is achieved for R=4 above approximately 1.0 sec for the two acausal filters (*Panel b* of Figures 5b and 5c). The relatively large variability introduced by the causal filter prevents drawing any statistically significant inference for R=4 with a sample size of twenty records.

In the elastic response case, as expected, the descending trend in the spectra ratio occurs only in the neighborhood of the corner period, $1/f_{HP,}$ and longer. The results for the inelastic response cases, however, show clearly that the descending trend leaks to periods much shorter than $1/f_{HP}$. This can be explained by the observation that the effective period of the inelastic oscillators is longer than the initial (elastic) period due to the lengthening effect caused by the post-elastic nonlinear behavior. The effective period at which an oscillator responds depends on the level of ductility reached. For the bilinear SDOF systems with 2% post-yield hardening used in this study, Figure 6 shows typical values of the displacement ductility ratio, μ, for constant values of R equal to 2, 4, and 8. The median values of μ in Figure 6 were used to compute the equivalent period, T', of SDOF systems with various initial (elastic) natural periods (Table 6) using, for example, the approach suggested by Kwan and Billington [10]. From Table 6, it can be seen that, for example, the effective period for a 0.5 sec SDOF system in an R=8 analysis on average increases by a factor of about 4 becoming about 2 sec. Similarly a 1s SDOF system in an R=8 case has an effective period of more than 3 sec. At 2 to 3 sec, the records processed with a corner frequency of 1.5 x f_{HP} are, on average, more deficient than those processed using f_{HP} because part of the signal at long periods in the former case has been filtered out. The lengthening of the effective period of vibration of inelastic SDOF oscillators is, therefore, fully consistent with the trend of the median spectral ratio curves (Figures 5a, 5b, and 5c) that decrease systematically from one for large R values. Boore and Akkar [1] reached similar conclusions for Butterworth causally filtered records. The results shown in Figures 5a through 5c show that the same phenomenon seems to also occur for both types of acausal filters considered here.

Sensitivity Analysis: Removal or Preservation of Residual Static Displacement

In this section the effect of removing or retaining the final static ground displacement in the raw ground motion records on time histories and elastic and inelastic spectra is investigated. Unlike the previous sensitivity cases, which were based on analysis of twenty normal component records and 21 parallel component records, this sensitivity analysis is based on records from three earthquakes and just six stations in the case of normal components and seven stations in the case of parallel components (see Table 2). It is emphasized that the accelerograms included in this suite, recorded within 5 km from the fault rupture, are characterized, on average, by residual static displacements (see Table 7) that are larger (and for some records, significantly so) than those for average near-source or far-field ground motion records. Therefore the results that are presented hereafter should be read in this light. A systematic study on the effects of removal or preservation of residual static displacement that comprises randomly selected records is left to future research.

Each record was processed in three different ways: (a) baseline corrected and LP filtered, but otherwise left unchanged, with a procedure that preserves the residual (static) displacement (Row 11); (b) causally filtered using a 4-pole filter (Row 6); and (c) acausally filtered using a 4-pole filter (Row 4). To preserve static displacements and correct for instrument malfunctions that distort tectonic displacements, we have used the methodology suggested by Grazier [5] and Boore [11] [12] to perform the baseline correction of the recorded motions. For this procedure, a least-square fit is performed on the original integrated velocity time history using three different functional forms. The first functional form is a simple linear trend in velocity. The second function is a bilinear function which is piecewise continuous and the last function is a simple

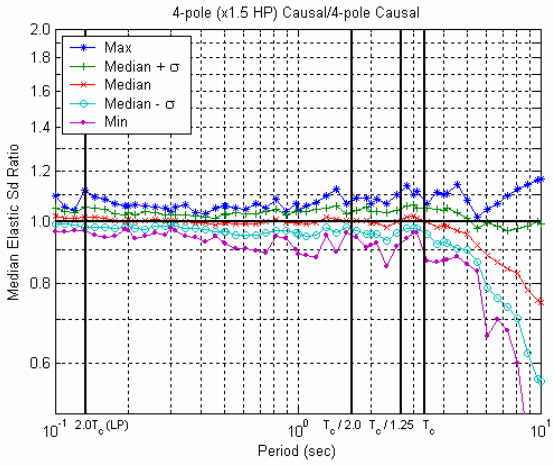

(a) R = 1 (Elastic)

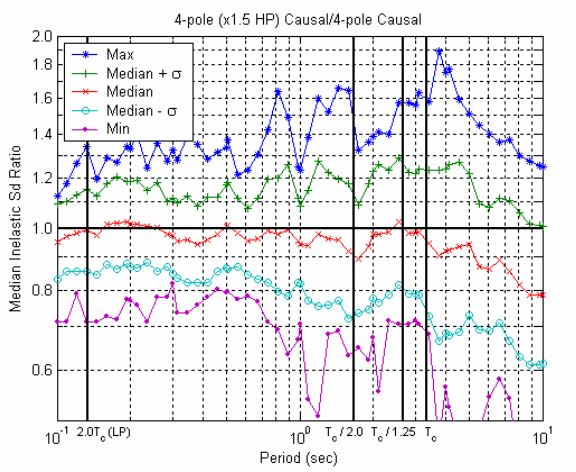

(b) R = 4

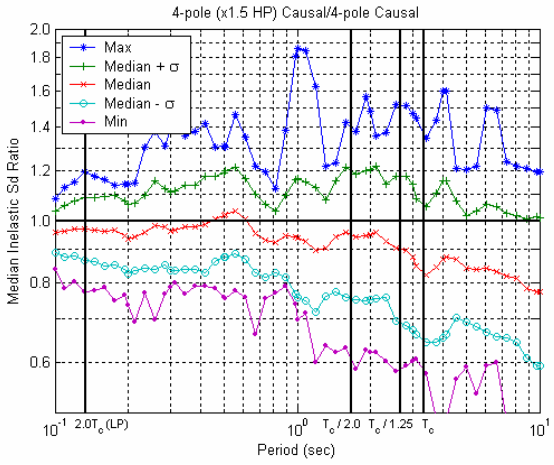

(c) R = 8

Figure 5a. ***High-pass corner frequency comparison*. Ratio of elastic (*Panel a*) and inelastic displacement response spectra (*Panel b, Panel c*) computed using a Butterworth 4-pole causal filter with two different values of the HP corner frequency. The statistics are computed across 20 records (normal component only). The vertical line labeled T_c/1.25 is the only one relevant here. Note that the value of Tc here has been adjusted to reflect the increase in the f_{HP} value. All the response spectra were created using records in Row 7 (i.e., 4-pole causal and 1.5 x HP) and Row 6 (i.e., 4-pole causal) in Table 2 (i.e., *Row 7/Row 6*).**

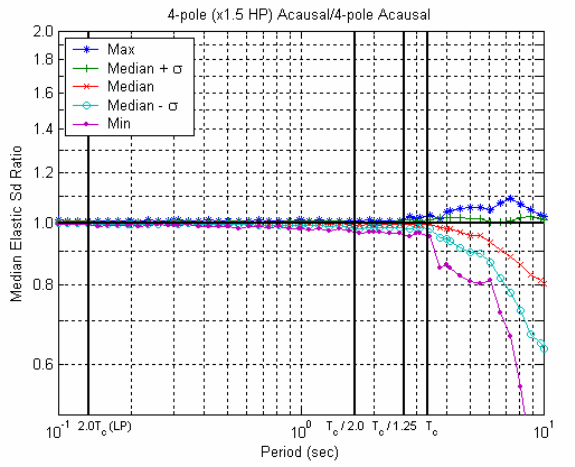

(a) R = 1 (Elastic)

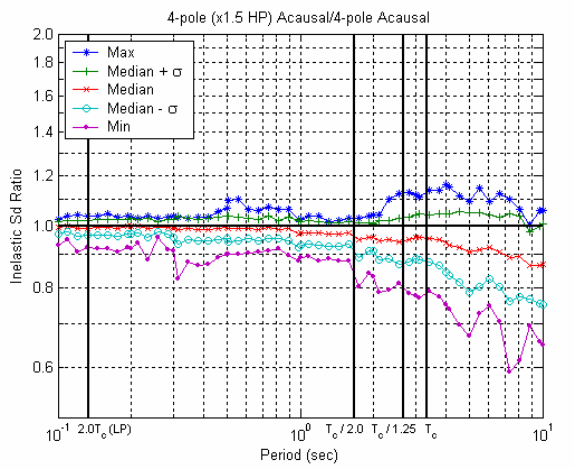

(b) R = 4

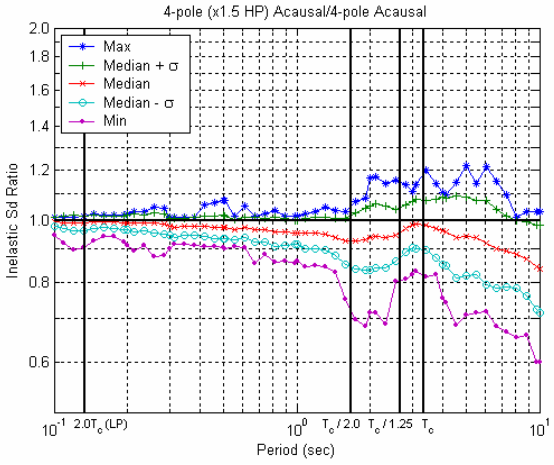

(c) R = 8

Figure 5b. ***High-pass corner frequency comparison*. Ratio of elastic (*Panel a*) and inelastic displacement response spectra (*Panel b, Panel c*) computed using a Butterworth 4-pole acausal filter with two different values of the HP frequency. The statistics are computed across 20 records (normal component only). The vertical line labeled T_c is the only one relevant here. Note that the value of Tc here has been adjusted to reflect the increase in the $f_{HP.}$ value. All the response spectra were created using records in Row 5 (i.e., 4-pole acausal and 1.5 x HP) and Row 4 (i.e., 4-pole acausal) in Table 2 (i.e., *Row 5/Row 4*).**

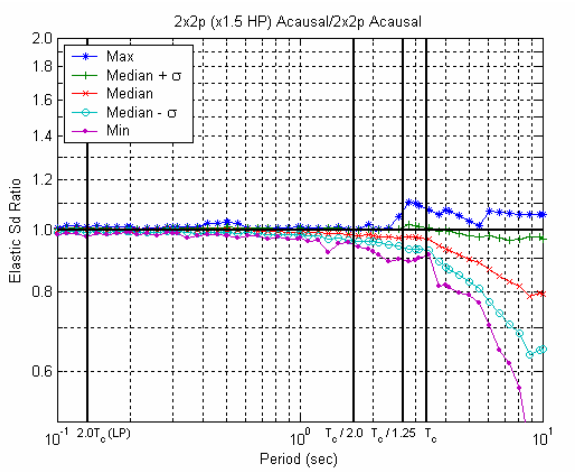

(a) R = 1 (Elastic)

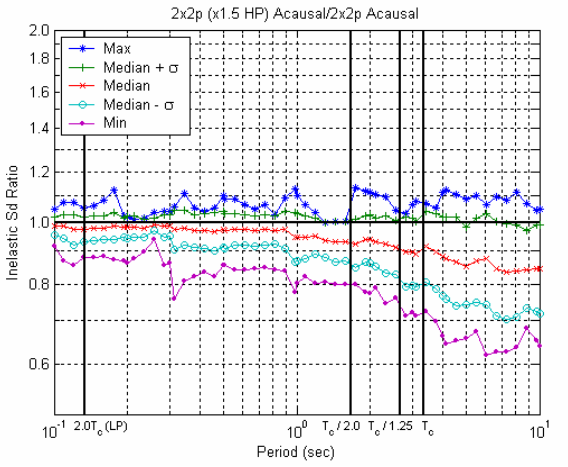

(b) R = 4

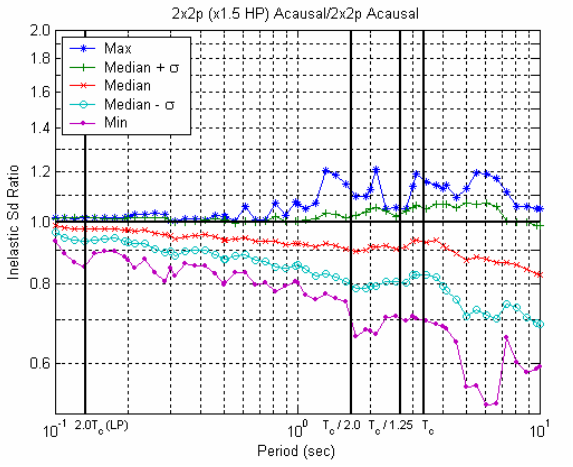

(c) R = 8

Figure 5c. ***High-pass corner frequency comparison*. Ratio of elastic (*Panel a*) and inelastic displacement response spectra (*Panel b, Panel c*) computed using a Butterworth 2-pole/2-pole acausal filter with two different values of the HP frequency. The statistics are computed across 20 records (normal component only). The vertical lines labeled $T_c/2.0$ and $2.0T_c$(LP) are the only ones relevant here. Note that the value of Tc here has been adjusted to reflect the increase in the f_{HP} value. All the response spectra were created using records in Row 2 (i.e., 2-pole/2-pole acausal and 1.5 x HP) and Row 1 (i.e., 2-pole/2-pole acausal) in Table 2 (i.e., *Row 2/Row 1*).**

Table 5. Summary of *high-pass corner frequency sensitivity analysis*. The statistics reported in *Panels b-c* are averaged across frequency (within usable bandwidth only). The values in *Panel b* bracket the statistics found for R=2 and R=4 for normal components. The standard deviation, s, is computed in natural logarithm terms and, therefore, is numerically close to the coefficient of variation (for values less than about 0.3). This table should be considered in conjunction with Figures 5a, 5b, and 5c.

Case	Normal					Parallel				
	PGA	PGV	PGD	Arias	T_D	PGA	PGV	PGD	Arias	T_D
4-pole (x1.5 HP) Causal/4-pole Causal	0.992	0.963	0.855	0.995	1	0.99	0.957	0.839	0.992	0.997
4-pole (x1.5 HP) Acausal/4-pole Acausal	0.999	0.958	0.857	0.995	1	0.998	0.934	0.854	0.992	0.998
2x2p (x1.5 HP) Acausal/2x2p Acausal	0.998	0.939	0.79	0.983	1	0.996	0.926	0.711	0.982	1

(a) Median ratios of ground motion parameters

Case	R = 1 (Normal)				R = 8 (Normal)			
	Min.	Max.	Med.	σ	Min.	Max.	Med.	σ
4-pole (x1.5 HP) Causal/4-pole Causal	0.850	1.121	0.999	0.033	0.58	1.863	0.956	0.159
4-pole (x1.5 HP) Acausal/4-pole Acausal	0.950	1.021	0.998	0.006	0.683	1.17	0.969	0.051
2x2p (x1.5 HP) Acausal/2x2p Acausal	0.921	1.028	0.995	0.009	0.749	1.201	0.944	0.067

(b) Statistics of ratios of elastic (R=1) and inelastic (R=8) response spectra for normal components

Case	R = 4 (Normal)				R = 4 (Parallel)			
	Min.	Max.	Med.	σ	Min.	Max.	Med.	σ
4-pole (x1.5 HP) Causal/4-pole Causal	0.508	1.658	0.969	0.167	0.512	1.634	0.968	0.166
4-pole (x1.5 HP) Acausal/4-pole Acausal	0.769	1.129	0.98	0.043	0.726	1.168	0.978	0.041
2x2p (x1.5 HP) Acausal/2x2p Acausal	0.758	1.129	0.969	0.056	0.635	1.394	0.963	0.082

(c) Statistics of ratios of inelastic (R=4) response spectra for normal and parallel components

quadratic in velocity. The best fitting velocity function is then differentiated to produce an acceleration trace, which is then removed from the recorded acceleration time history.

The fitting process has been automated such that, after the starting time point for the velocity fit has been selected, all linear, bilinear, and quadratic segments are fitted and their standard errors ranked [3]. The "best fit" is then viewed for reasonableness, a qualitative assessment based on a constant, or nearly constant, overall level of permanent (static) displacement. A suite of starting times is marched through resulting in a fairly rapid and exhaustive evaluation of the most appropriate correction function for each component. This processing approach, to maintain static displacements, suffers the same uncertainty or non-uniqueness as more typical processing schemes, which remove low frequency noise by high-pass filtering. Unless there are independent sources of information, such as co-located Global Positioning System sensors for the case of recovering static displacements, or estimates of low-frequency noise levels for the case of HP filtering, the selection of processing parameters relies on judgment. The corrected time histories are then LP filtered to remove potential high frequency noise. The LP filters are causal Butterworth, using the same corner frequencies as in the PEER processing (typically near 50 Hz). Both the causal and acausal filters (cases b and c) remove the final displacement offset. Results of this sensitivity analysis are presented in Table 8 and Figures 7a and 7b.

The preservation or removal of the residual static offset from the ground motion records has a remarkable effect on the values of PGD and PGV and a smaller effect on PGA, AI, and T_d (on average,

Table 6. Equivalent post-yielding period, T', of an SDOF system with initial elastic natural period of 0.2 sec, 0.5 sec, 1.0 sec, and 2.0 sec for different levels of ductility ratio, *m*. The *m* values correspond to the median values shown in Figure 6 for different levels of R. The values of T' were computed using the procedure suggested by Kwan and Billington [10] that is based on the secant stiffness method.

	T = 0.2s		T = 0.5s		T = 1s		T = 2s	
R	μ	T' (s)	μ	T' (s)	μ	T' (s)	μ	T' (s)
2	3.12	0.35	2.30	0.75	1.96	1.39	2.04	2.83
4	14.28	0.67	7.35	1.28	5.00	2.15	4.30	4.02
8	48.53	1.00	21.82	1.96	12.02	3.14	9.85	5.79

Table 7. Static residual displacements for the six fault-normal components and the seven fault-parallel components considered here. The fault-normal component at the Sakarya station is not available.

		Static Residual Displacement (cm)	
Earthquake	**Station**	**Normal Component**	**Parallel Component**
Landers	Lucerne	193.5	71.7
Kocaeli	Izmit	43.0	15.2
Kocaeli	Yarimca	166.6	70.0
Kocaely	Sakarya	N/A	178.2
Chi-Chi	TCU049	13.2	27.2
Chi-Chi	TCU052	14.4	46.0
Chi-Chi	TCU068	497.4	713.8

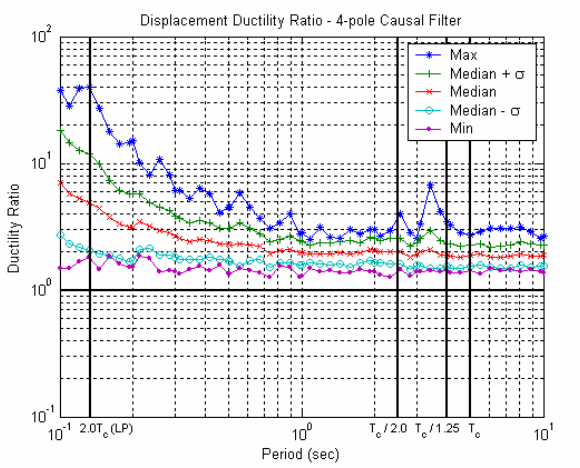

(a) R = 1 (Elastic)

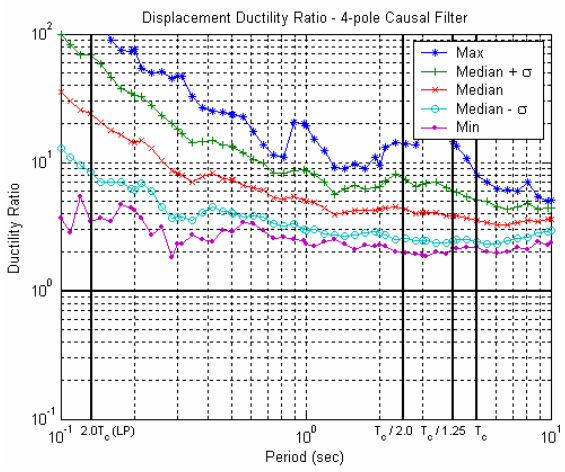

(b) R = 4

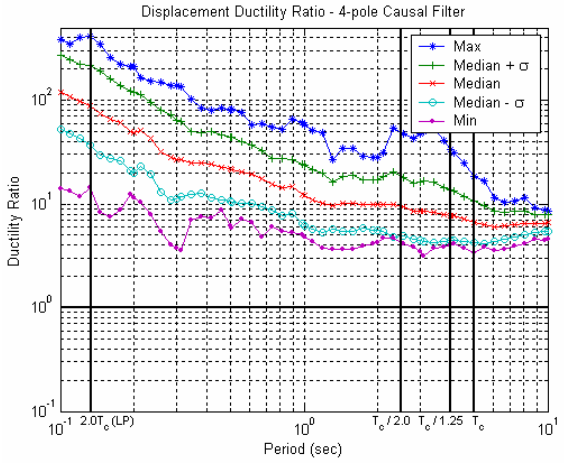

(c) R = 8

Figure 6. Displacement ductility ratio of SDOF systems of different natural periods for constant R values of 2, 4, and 8. The curves were created by running the 20 normal components processed using the Butterworth 4-pole causal filter. Note that large values of the ductility ratio may not be realizable in real structures.

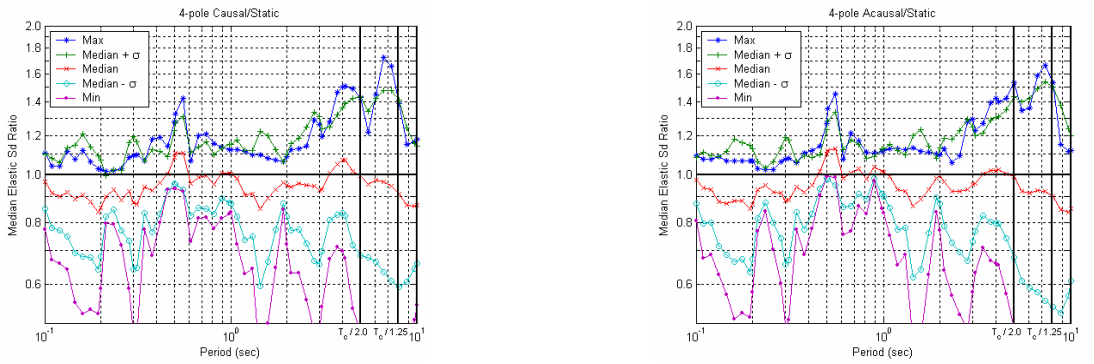

(a) R = 1 (Elastic)

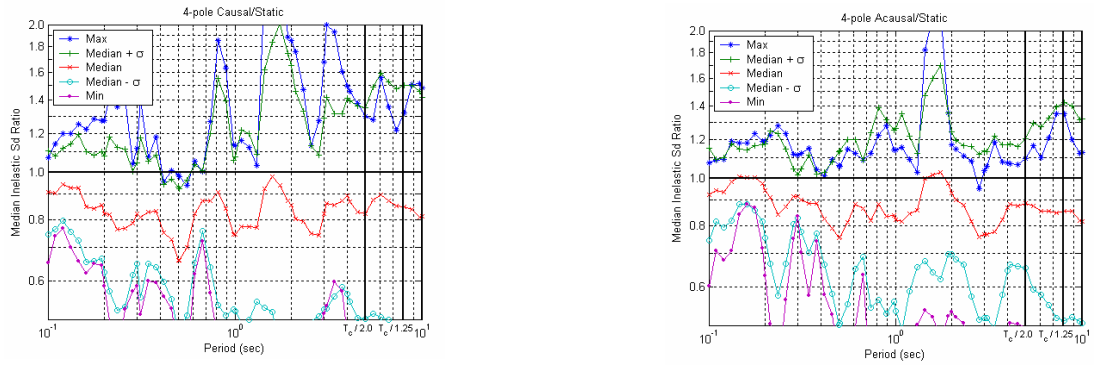

(b) R = 4

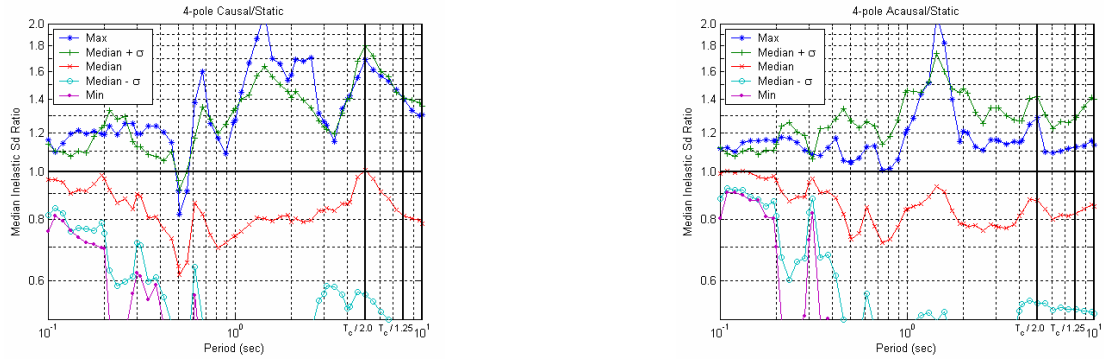

(c) R = 8

Figure 7a. ***Static vs. no-static displacement comparison (normal components).*** **Ratio of elastic (*Panel a*) and inelastic displacement response spectra (*Panels b* and *c*). The spectra in the numerator of the ratio displayed in the three figures on the left are computed using a 4-pole causal filter (*Row 6*) and those in the three figures on the right are computed using a 4-pole acausal filter (*Row 4*). Both filters remove the static displacement from the input motions. The records that generate the spectra in the denominator for all cases are baseline-corrected and low-pass filtered but the final static offset is preserved (*Row 11*). The statistics are computed across 6 records only. The vertical line labeled $T_c/1.25$ is the relevant one in the three figures on the left. The suggested usable bandwidth in the three figures on the right goes up to 10 sec.**

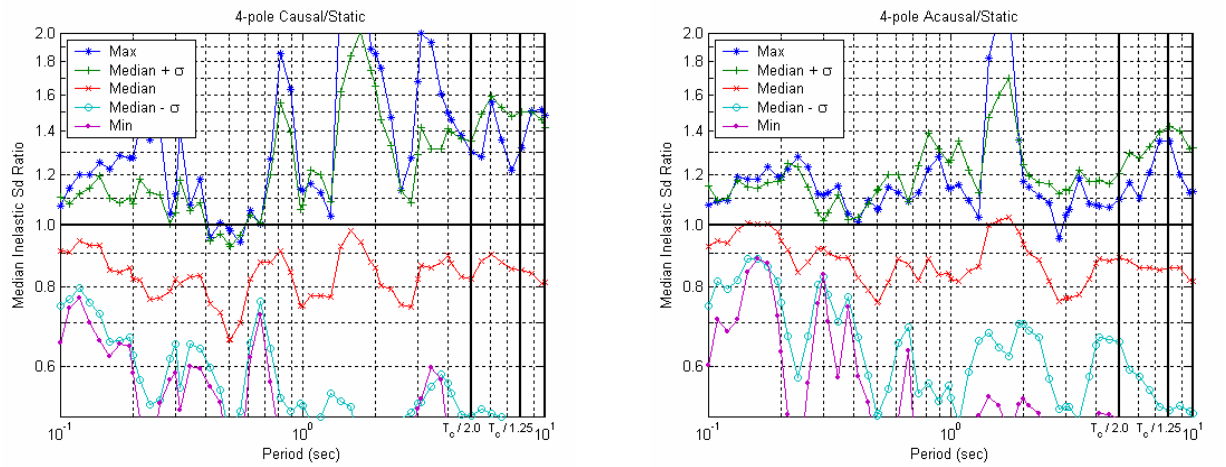

(a) Normal components (R = 4)

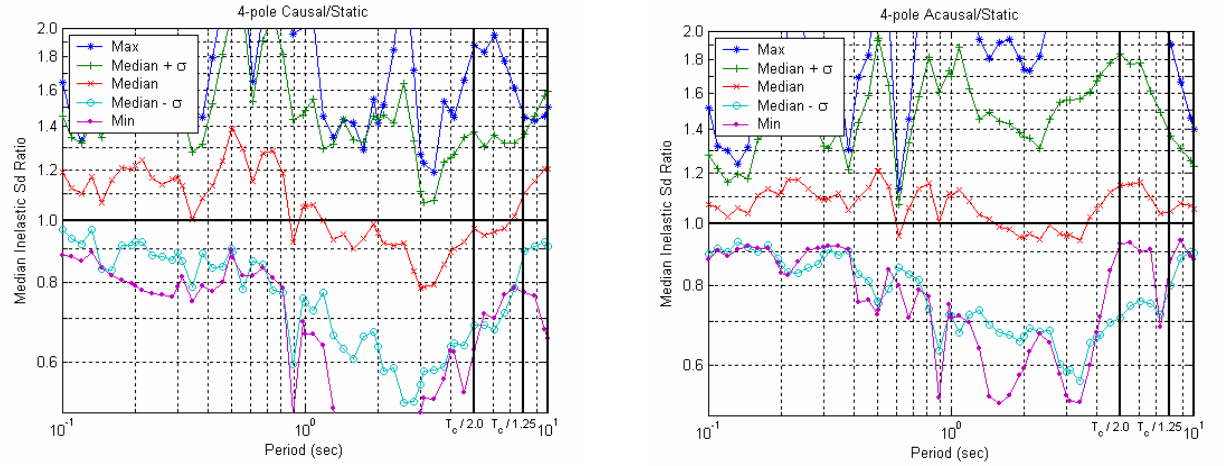

(b) Parallel components (R = 4)

Figure 7b. ***Static vs. no-static displacement comparison — normal vs. parallel components*.** **Ratio of inelastic displacement response spectra (R = 4) computed using the normal (*Panel a*) and parallel component (*Panel b*) records for the stations listed in Table 2, Row 11. The spectra in the numerator in the two figures on the left are computed using a 4-pole causal filter (*Row 6*) and those in the two figures on the right are computed using a 4-pole acausal filter (*Row 4*). Both filters remove the static displacement from the input motions. The records that generate the spectra in the denominator are only baseline-corrected and the final static offset is preserved (*Row 11*). The statistics are computed across six records for the normal components and seven records for the parallel components. The vertical line labeled $T_c/1.25$ is the only one relevant in the two figures on the left whereas the suggested usable bandwidth goes up to 10s in the two figures on the right.**

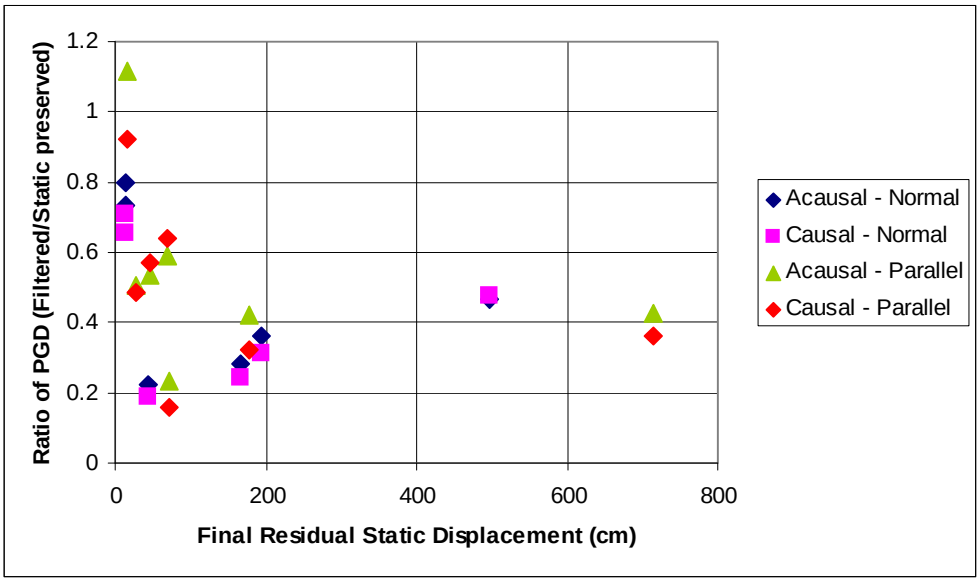

Figure 7c. For each record the ratio of PGD with residual displacement removed to PGD with residual displacement preserved is plotted versus the final residual displacement. These ratios are shown for both causal and acausal filters.

below 10%). As it can be seen from Figure 7c, the PGD values for records with the static displacement removed are, on average, less than half of those obtained for records where the static offset is preserved. This comment holds regardless of the causality of the filter and the orientation of the component records. Similarly, the PGV values drop, on average, by 15% to approximately 20% for the fault-normal component case, and by 5% to 10% for the fault-parallel component case. The upper-bound values refer to the records processed with the causal 4-pole filter while the lower-bound values refer to the acausal 4-pole filter. Figure 8 shows the significant effect of removing or preserving the residual static offset on the ground displacement component time histories at one station for each of the three earthquakes (i.e., Landers, Kocaeli, and Chi-Chi) represented in this dataset. The pre-event motions or ramps resulting from the acausal filters are evident while the causal filters maintain the arrival times of significant displacements. In some cases (e.g., LCN, parallel and TCU068, normal) peak displacements are nearly of opposite polarity between the causal and acausal processing. While not the subject of this study, these features may have implications for analyses of multidimensional structures, as well as extended multi-support structures where phasing between components and supports may be an issue. It seems reasonable to assume that any analyses that may be sensitive to phasing between components and stations (e.g., spatial coherence) would benefit from processing which maintained causality, particularly if different corner frequencies between components or stations were selected to maximize useable bandwidths.

The most important consideration stemming from the results in Figure 7a, which shows normal component results only, is the significant effect that the removal of the static offset has on the elastic and, more so, the inelastic displacement response spectra across a wide range of periods. Not only is the long period range affected (i.e., periods of 4 to 6 seconds, which is approximately the time it takes for the static offset to build-up) but also the period range of the response spectra many multiples shorter (e.g., 0.5 sec to 1.0 sec). The median curve for the ratio of inelastic displacement response spectra computed without and

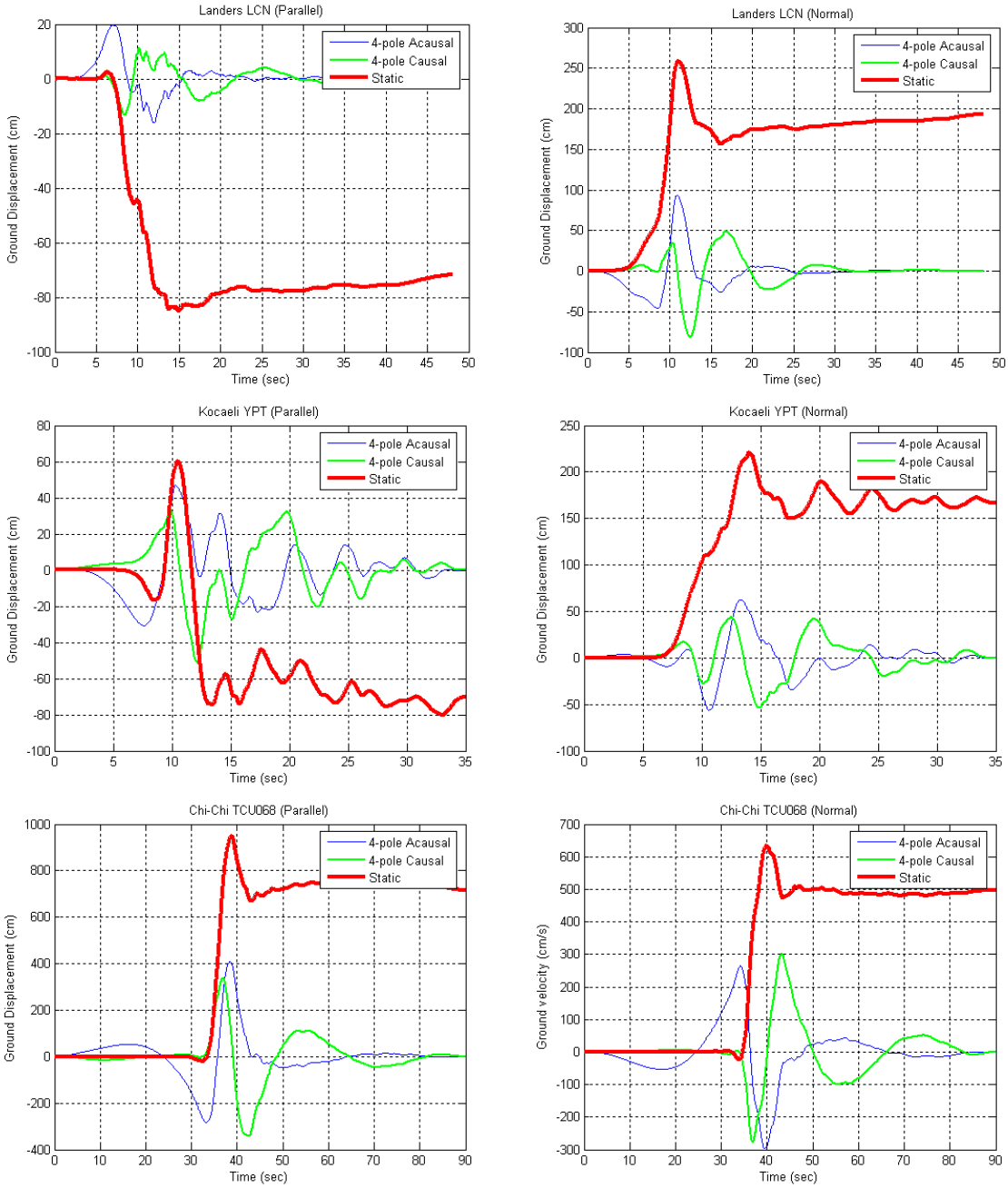

Figure 8. **Ground displacement time histories for the normal and parallel components recorded at one station for each of the three earthquakes used in this sensitivity analysis. The time histories in which the static offset was removed were processed using a 4-pole causal filter (*Row 6*) and a 4-pole acausal filter (*Row 4*). The records in which the final static displacement (called "Static" in the figures) was retained were baseline-corrected and low-pass filtered (*Row 11*). The phase distortion introduced by the causal filter and the pre-event transients caused by the acausal filter are particularly evident.**

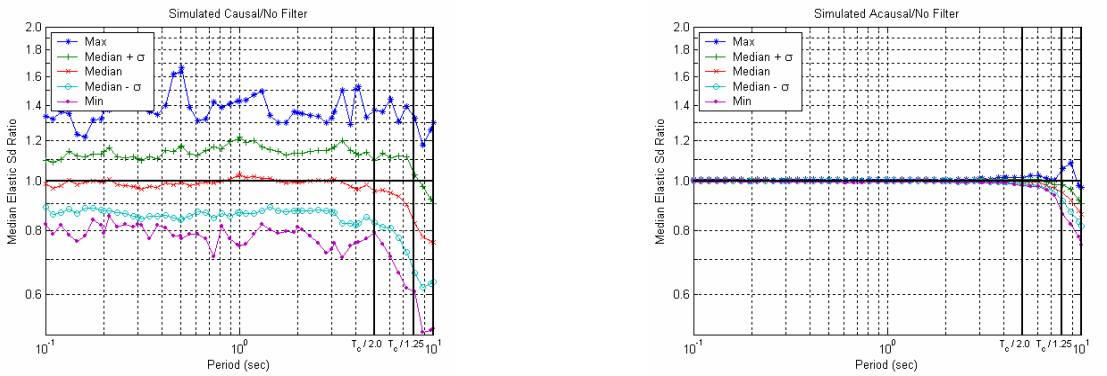

(a) R = 1 (Elastic)

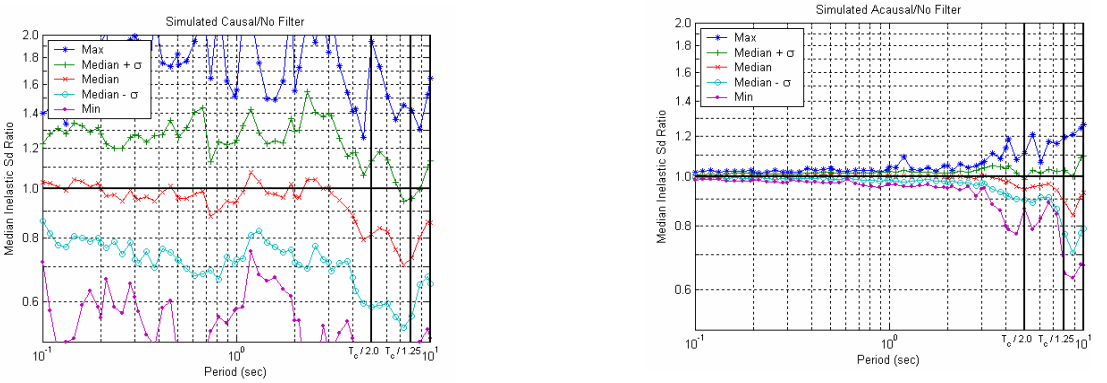

(b) R = 4

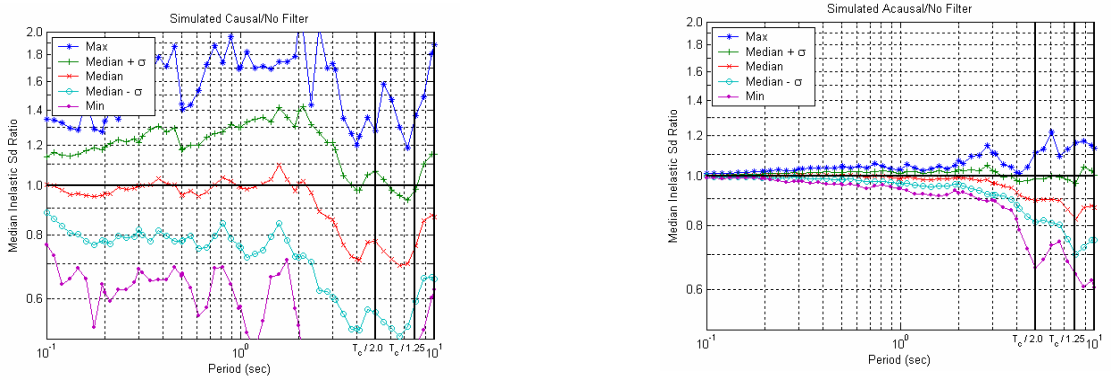

(c) R = 8

Figure 9. ***Simulated records – Filter vs. no-filter*****. Ratio of elastic (*Panel a*) and inelastic displacement response spectra (*Panels b* and *c*). The spectra in the numerator in the three figures on the left were computed using a causal filter (*Row 13*) and those in the three figures on the right were computed using an acausal filter (*Row 12*). The records that generated the spectra in the denominator were unfiltered (*Row 14*). The statistics are computed across 30 records (average components). The vertical line labeled $T_c/1.25$ defines the boundary of the suggested usable bandwidth in the three figures on the left-hand side whereas the usable bandwidth goes up to 10s (i.e., $T_c/1.0$) in the three figures on the right-hand side.**

with the static offset drops to values of 0.7 to 0.8 and even lower at some moderate periods. Because of the limited sample size, however, these results are not statistically significant at any customary level. Recall that the standard deviation of the mean is equal to s, whose value can be estimated from Figure 7a, divided by the square root of the sample size, *n* (here *n* is equal to the number of records, i.e., 6). Therefore, a typical spectrum ratio equal to 0.90 to 0.95 for R=1 is only about one sigma away from unity for typical values of s around 0.15 to 0.20.

The comments reported above, however, seem to hold only for the normal component of ground motion. Inspection of Figure 7b, which displays the inelastic displacement response spectra ratios for R=4 (fault-parallel components), shows that removing the residual static displacement from the input time history does not result in an unconservative response, on average. Again, the sample size of seven records is too small to make statistically sound inferences. Further research with more populated record database is needed to clarify this issue.

Although these results are affected by large statistical uncertainty due to the limited sample size and, therefore, are not statistically significant at any customary level, they are of considerable interest at least for extreme cases such as those included in this small suite of records. The static offset is often thought to have a negligible effect on the response of most structures of engineering interest and, therefore, current practice seldom includes it in structural response time history analysis. From the results shown here, we infer

Table 8. **Summary of *static vs. no static displacement sensitivity analysis*. The statistics reported in *Panels b-c* are averaged across frequency (within usable bandwidth only). The values in *Panel b* bracket the statistics found for R=2 and R=4 for normal components. The standard deviation, s, is computed in natural logarithm terms and, therefore, is numerically close to the coefficient of variation (for values less than about 0.3). This table should be considered along with Figures 7a and 7b**.

Case	Normal					Parallel				
	PGA	PGV	PGD	Arias	T_D	PGA	PGV	PGD	Arias	T_D
4-pole Acausal/Static	0.911	0.846	0.429	0.956	1.03	1.055	0.951	0.497	1.038	0.954
4-pole Causal/Static	0.941	0.778	0.384	0.956	1.03	1.088	0.893	0.436	1.037	0.959

(a) Median ratios of ground motion parameters

Case	R = 1 (Normal)				R = 8 (Normal)			
	Min.	Max.	Med.	σ	Min.	Max.	Med.	σ
4-pole Acausal/Static	0.322	1.666	0.95	0.23	0.22	2.095	0.852	0.412
4-pole Causal/Static	0.422	1.725	0.954	0.22	0.241	2.106	0.836	0.431

(b) Statistics of ratios of elastic (R=1) and inelastic (R=8) response spectra for normal components

Case	R = 4 (Normal)				R = 4 (Parallel)			
	Min.	Max.	Med.	σ	Min.	Max.	Med.	σ
4-pole Acausal/Static	0.299	2.234	0.877	0.324	0.522	3.365	1.067	0.33
4-pole Causal/Static	0.326	2.79	0.831	0.393	0.413	2.661	1.055	0.338

(c) Statistics of ratios of inelastic (R=4) response spectra for normal and parallel components

Table 9. Summary of *simulated records – filter vs. no filter sensitivity analysis*. Statistics of ratios of elastic and inelastic response spectra for simulated records (average component). The statistics reported in *Panels b-c* are averaged across frequency (within usable bandwidth only). The standard deviation is computed in natural logarithm terms and, therefore, is numerically close to the coefficient of variation (for values less than about 0.3). This table should be considered in conjunction with Figure 9.

Case	Average				
	PGA	PGV	PGD	Arias	T_D
Simulated 5-pole Acausal/No Filter	1	0.976	0.833	0.999	1.001
Simulated 5-pole Causal/No Filter	1	0.989	0.818	0.977	0.994

(a) Median ratios of ground motion parameters

Case	R = 1				R = 4			
	Min.	Max.	Med.	σ	Min.	Max.	Med.	σ
Simulated 5-pole Acausal/No Filter	0.747	1.081	0.991	0.007	0.631	1.264	0.986	0.034
Simulated 5-pole Causal/No Filter	0.616	1.666	0.986	0.144	0.364	2.372	0.954	0.28

(b) Statistics of ratios of elastic (R=1) and inelastic (R=4) response spectra

Case	R = 8			
	Min.	Max.	Med.	σ
Simulated 5-pole Acausal/No Filter	0.603	1.217	0.969	0.042
Simulated 5-pole Causal/No Filter	0.33	2.108	0.932	0.259

(c) Statistics of ratios of inelastic (R=8) response spectra

that this practice may be unconservative for structures located very close to the causative faults where large residual static displacements may occur. This effect is expected not to be important for structures farther away from the causative fault. A larger sample size of ground motion records is, however, necessary to confirm or disprove these results.

Effect of Filtering Simulated Ground Motions on Response Spectra

This section focuses on the effect on elastic and inelastic response spectra of filtering synthetic ground motion records with a 5-pole Butterworth causal and a 5-pole Butterworth acausal filter. Given the limited resources for this project, we used a set of simulated records that were already available. The HP and LP corner frequencies, as well as other details about this suite of simulated records, were included in Table 2. As discussed in the introductory motivation section, one can argue that the response spectra derived from unfiltered synthetic records provide a benchmark for the spectra derived from the filtered signals. Results are presented in Table 9and Figure 9.

Inspection of Table 9 (*Panel a*) shows that the application of a filter does not materially alter, on average, the values of PGA but it reduces (by about 20%) the values of PGD and to a much lower extent the values of PGV. Figure 9 shows that both the causal filter (*Panels a, b,* and *c, left*) and acausal filter (*Panels a, b,* and *c, right*) do not introduce any significant bias in the response spectra up to a moderately long period. The period above which significant bias occurs decreases as the level of nonlinearity increases (i.e., R in-

creases). The more severe the post-yielding deformation of the SDOF system is (deformation that increases with the R value), the more the effective oscillation period lengthens into a range where part of the signal is filtered out. Hence, at long periods the application of a causal or acausal filter generates records that are, on average, more benign with respect to the structural response they induce than the corresponding unfiltered records. This is more so for the causally filtered records. The threshold period is in excess of 3.0 sec for R=4 and approximately 2.0 sec for R=8.

Finally, what is strikingly evident from Figure 9 is the similarity between the displacement response spectra of the unfiltered records and that of the acausally filtered records as shown by the small variability in the spectral ratios in the right-hand side of *Panels a, b and c*. This lower variability as compared to the causally filtered records (left-hand side of Figure 9) suggests superiority of acausal filters, considering only this aspect of tradeoffs between causal and acausal filters.

CONCLUSIONS

This study examined the effects of several ground-motion filtering techniques on

- The elastic and inelastic response spectra of bilinear SDOF systems with non-degrading strength and stiffness, and with periods ranging from 0.1 sec to 10 sec, and
- A suite of conventional scalar ground motion parameters of the filtered time histories.

These effects were quantified for filtering techniques and filter parameter values (e.g., corner frequencies) commonly used in current practice for typical strong-motion records. It should be understood, however, that some of these results might not hold true for other records not considered here.

In general, for the cases considered in this study the following conclusions can be made:

1. For all filters the long-period part of the spectra is more sensitive to the filter characteristics and this effect tends to increase with the severity of the nonlinear response (i.e., increasing R values).
2. Among the parameter variations considered here, the removal or preservation of the residual static displacement has the largest impact, at least for this limited pool of ground motions recorded within 5 km from the causative fault. The ground motions with static residual displacement preserved seem to cause more severe nonlinear response of structures with a wide range of natural periods (even much shorter than the typical rise time of the static displacement offset). We expect, however, this effect to be less noticeable on more standard accelerograms recorded farther away from the fault where the residual displacements tend to be more limited. Also this effect was found to be more severe in the fault-normal than in the fault-parallel records. Further research is needed to investigate this issue more in depth.
3. The value of the HP corner frequency, f_{HP}, also had a visible effect on the linear and nonlinear response spectrum ratio. Records that are filtered with a larger value of the HP corner frequency tend to be more benign if used to compute the nonlinear response of oscillators with periods even much lower than the reciprocal of the value of f_{HP}

used. The post-yielding period lengthening of oscillators is responsible, at least in part, for this effect. Among the ground motion parameters considered here, only PGD and, to a lesser extent, PGV, are affected by the different aspects of the filtering technique. It should be emphasized, however, that these conclusions are valid for the typical values of the HP and LP corner frequencies used here, values which are in line with those commonly used in current practice for typical strong-motion records.

4. The short study involving a suite of synthetic records has suggested that the use of acausal filters may be preferable over the use of causal filters. This conclusion is based on the assumption that one can consider the unfiltered records as being "true", noiseless signals.

The details of the effects on spectra and ground motions caused by the different filtering techniques and variations of parameter values of the filters are reported below:

- *Causality of the filter*. The elastic and inelastic displacement response spectra associated with ground motion records that have been causally filtered are, on average, statistically indistinguishable from the spectra of acausally filtered records with filters of the same order and corner frequencies. Also, there is virtually no statistical difference in response spectra within the suggested bandwidth limit of the filters when records are acausally filtered with either a single filter or a cascade filter. The record-to-record variability of response spectra ratios is significantly larger for the causal/acausal case as compared to the acausal/(cascade acausal) case. This is because causal filters alter the record phases while acausal filters, regardless of the order, do not. The variability of the spectral ratio increases for both causally and acausally filtered records with severity of nonlinear behavior and, for a given level of nonlinearity, it tends to increase with period. The values of PGD and PGV are sensitive to the causality of the filter. The acausal 4-pole filter appears to generate PGD and PGV values that are, on average, larger by about 5% than those produced by the causal 4-pole filter and the cascade acausal 2-pole/2-pole filter. Other ground motion parameters such as PGA, AI, and Trifunac bracketed duration, T_d, are virtually insensitive to the causality of the filter.
- *Filter order*. Changing the filter order (from fourth- to fifth-order) does not significantly affect the elastic and inelastic displacement response spectra for both causal and acausal filters. Ground motion parameters are also not affected.
- *Sensitivity to high-pass corner frequency*. Increasing the high-pass corner frequency, f_{HP}, by a factor of 1.5 causes the elastic and inelastic spectra to systematically decrease across virtually *the entire frequency range*, not just in the vicinity of f_{HP}. PGD and PGV values are also decreased, on average, when the typical values of the HP corner frequencies for a suite of records used here is multiplied by a factor of 1.5. The other ground motion parameters (PGA, AI, and T_d) are virtually unaffected by the selection of f_{HP}.
- *Sensitivity to residual static displacement*. Removing the residual static displacement from a ground motion record with *large* residual displacement, such as those considered here, generates inelastic displacement response spectra that appear, on average, to be 10% to 20% lower at mild to moderate levels of nonlinear behavior than

spectra with static offset preserved. For severely inelastic behavior (R=8) the spectra with static offset removed can be up to 30% lower. This phenomenon was observed for the fault-normal components only. These results, however, are not statistically significant at any customary level due to the limited number of records used in this study. PGD and PGV are also significantly affected by the removal of static offset. PGV drops, on average, 25% to 30% while PGD drops more than 50% when the static displacement is removed from ground motion records.

- *Filtering synthetic records*. Filtering of synthetic records with a causal or acausal filter has, on average, no significant effect on displacement response spectra for periods up to approximately 2 sec. At longer periods the response spectra of filtered records are systematically lower than that of unfiltered records, as expected. The decreasing trend beyond 2 sec increases with oscillator period and with level of nonlinearity. The response spectrum ratios obtained by applying a 4-pole acausal filter exhibit much less variability with respect to the unfiltered records, compared to using a 4-pole causal filter. The conclusion that acausally filtered records may be superior to causally filtered stems exclusively from this observation, independent of other tradeoffs of desirable and undesirable features which exist between causal and acausal filtering.

REFERENCES

1. Boore, D.M., and S. Akkar (2003). Effect of causal and acausal filters on elastic and inelastic response spectra, *Earthquake Eng. Struct. Dyn.*, 32:1729-1748.

2. Boore, D.M. (2003). *Personal Communication*, Menlo Park, Calif.

3. Gregor, N., W. J. Silva, and R. Darragh, (2002). *Development of Attenuation Relations for Peak Particle Velocity and Displacement*, PEARL Report to PG&E, CEC, and Caltrans, June 12.

4. Somerville, P. G., N. F. Smith, R. W. Graves, and N. A. Abrahamson (1997). Modification of empirical strong ground motion attenuation relations to include the amplitude and duration effect of rupture directivity, *Seismo. Res. Lett.*, 68(1):199-222.

5. Grazier V. M. (1979). Determination of the true ground displacement by using strong motion records. Izvestiya Academy of Sciences, USSR, *Physics of the Solid Earth*, 15(12):875-885.

6. Boore, D. M., C. D. Stephens, and W. B. Joyner (2002). Comments on baseline correction of digital strong-motion data: Examples from the 1999 Hector Mine, California, earthquake, *Bull. Seismo. Soc. Am.*, 92(4):1543-1560.

7. Silva, W. J., N. A. Abrahamson, G. Toro, and C. Costantino. (1997). Description and validation of the stochastic ground motion model," Report Submitted to Brookhaven National Laboratory, Associated Universities, Inc. Upton, New York 11973, *Contract No. 770573*.

8. Silva, W. J., S. Li, R. Darragh, and N. Gregor (1999). *Surface geology based strong motion amplification factors for the San Francisco Bay and Los Angeles Areas*, A PEARL report to PG&E/CEC/Caltrans, Award No. SA2120 59652.

9. Silva, W. J., R. Darragh, N. Gregor, G. Martin, C. Kircher, and N. A. Abrahamson (2000). A reassessment of site coefficients and near-fault factors for building code provisions. Final Report *USGS Grant award #98-HQ-GR-1010*.

10. Kwan, W.-P., and S. Billington (2003). Influence of hysteretic behavior on equivalent period and damping of structural systems, *J. Struct. Eng.*, 129(5):576-585.

11. Boore, D. M. (1999). Effect of baseline corrections on response spectra for two recordings of the 1999 Chi-Chi, Taiwan, earthquake, *USGS Open File Report, 99-945*.

12. Boore, D. M. (2000). Effect of baseline corrections on displacements response spectra for several recordings of the 1999 Chi-Chi, Taiwan, earthquake, *Bull. Seismo. Soc. Am.*, 91(5):1199-1211.